GLOBAL BIOGEOCHEMICAL CYCLES, VOL. 14, NO. 1, PAGES 429-454, MARCH 2000

Factors governing the oceanic nitrous oxide distribution: Simulations with an ocean general circulation model

P. Suntharalingam

Earth and Planetary Sciences, Harvard University, Cambridge, Massachusetts.

J. L. Sarmiento

Program in Atmospheric and Oceanic Sciences, Princeton University, Princeton, New Jersey.

Abstract. A global model of the oceanic nitrous oxide distribution is developed to evaluate current understanding of the processes governing nitrous oxide formation and distribution in the open ocean. N_2O is treated as a nonconserved tracer in a global ocean general circulation model subject to biological sources in the oceanic interior and gas exchange at the ocean surface. A simple scalar parameterization linking N_2O production to oxygen consumption (and based on observed correlations between excess N_2O and apparent oxygen utilization) is successful in reproducing the large-scale features of the observed distribution, namely, high surface supersaturations in regions of upwelling and biological productivity, and values close to equilibrium in the oligotrophic subtropical gyres. The majority of the oceanic N_2O source is produced in the upper water column (over 75% above 600 m) and effluxes directly to the atmosphere in the latitude band of formation. The observed structure at depth is not as well reproduced by this model, which displays excessive N_2O production in the deep ocean. An alternative source parameterization, which accounts for processes which result in a depth variation in the relationship between N_2O production and oxygen consumption, yields an improved representation of the deep distribution. The surface distribution and sea-air flux are, however, determined primarily by the upper ocean source and, therefore, are relatively insensitive to changes in the nature of deep oceanic N_2O production.

1. Introduction

The current drive to identify the processes involved in the global nitrous oxide (N_2O) cycle and to constrain the atmospheric N_2O budget owes its impetus to the climatic implication of specific properties of the gas that have been uncovered in recent years. N_2O was first identified as an agent in stratospheric ozone depletion in 1970 [*Crutzen et al.*, 1970], and, following investigation of its radiative properties, is now also classified as an important greenhouse gas [*Ramanathan et al.*, 1985]. These characteristics, in combination with observations of its increasing concentration in the atmosphere [*Prinn et al.*, 1990] and long atmospheric lifetime (120 ± 30 years) [*Mahlman et al.*, 1986, *Prinn et al.*, 1990, *Ko et al.*, 1991] have highlighted its potentially significant climatic influence.

Paper number 1999GB900032.
0886-6236/00/1999GB900032$12.00

The majority of the source to the atmosphere is derived from bacterially mediated reactions in soils and water. These sources display a high degree of temporal and spatial variability; although they have been subject to recent intensive study, they are still not well quantified, and the governing cycling mechanisms are subject to some uncertainty. This study focuses on the processes responsible for marine N_2O formation and distribution in the open ocean and the resulting oceanic flux to the atmosphere. According to the most recent Intergovernmental Panel on Climate Change (IPCC) estimates, the oceanic flux constitutes a significant source of N_2O to the atmosphere, providing 1-5 Tg N out of a total annual source estimate of 10-17 Tg N [*Houghton et al.*, 1995]. However, the oceanic N_2O distribution displays a high degree of spatial and temporal variability which makes constraint of the global oceanic flux difficult. Furthermore, controversy still surrounds the issue of the dominant formation pathway; water column nitrification, during the subsurface oxidation of organic matter, has been widely accepted as the main source for the majority of the oceanic N_2O. This assumption has,

however, received challenges based on isotopic measurements and evidence that the N_2O cycle displays complex behavior in some oceanic environments.

We employ a combination of three-dimensional(3-D) numerical modeling and analysis of surface and deep N_2O data in this study to evaluate our current understanding of these processes and to quantify the net open oceanic source. The approach taken has been to develop simple parameterizations for N_2O formation based on recent interpretations of observational constraints, embed these in a model of realistic circulation, and evaluate the resulting global N_2O distribution against available observational data. In the next section we review the current state of knowledge on processes governing the marine nitrous oxide cycle and present the observational basis for our N_2O model parameterizations. Section 3 outlines the model components and configuration, and sections 4-6 discuss simulation results for the global N_2O distribution and net oceanic source.

2. Marine N_2O Cycle

2.1. Main Cycling Processes

The main biological pathways for marine N_2O cycling are via nitrification and denitrification processes, as summarized in Figure 1. N_2O is produced as an intermediate product in the process of biological denitrification which involves the bacterially mediated multistep reduction of nitrate to nitrogen gas [*Payne et al.*, 1971]. Not all strains of denitrifying bacteria are able to carry this process out to completion and produce N_2. Many lack the necessary enzymes to metabolize all of the intermediates and thus only participate in a subset of steps; for example, organisms lacking the enzyme nitrous oxide reductase will cause the process to terminate at N_2O, thus yielding a source of the gas. Since N_2O can also be consumed by denitrification processes (i.e., by being reduced to N_2), as well as being produced by them, denitrification can provide a net sink for N_2O

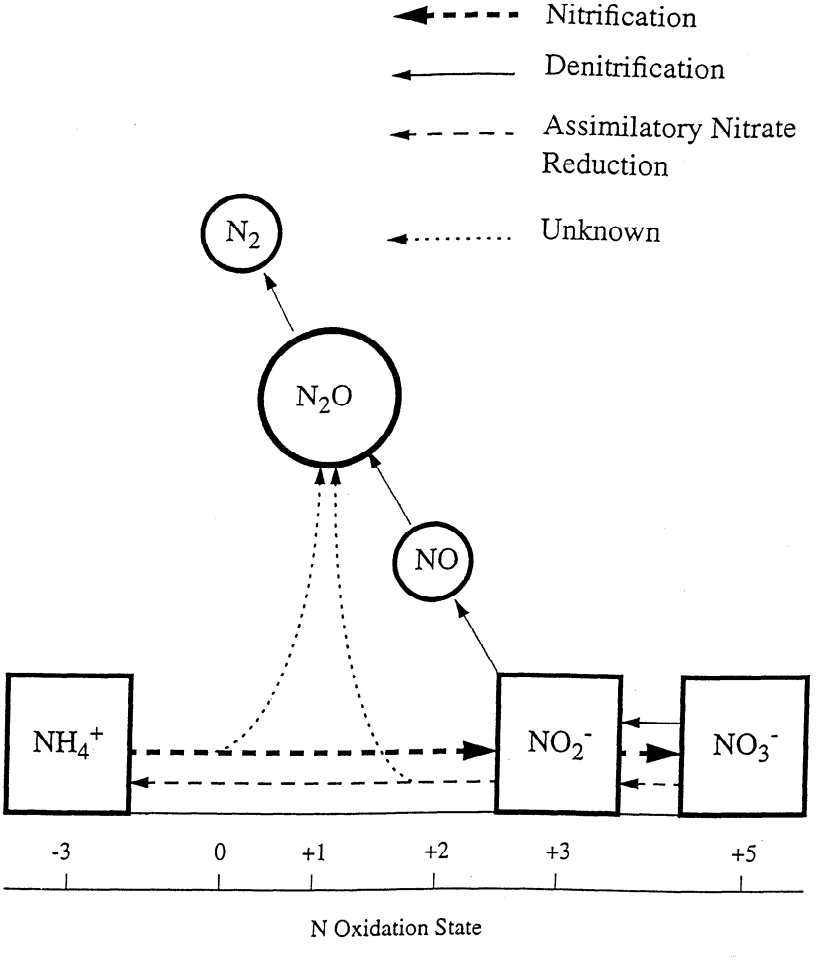

Figure 1. Bacterial nitrogen transformations involved in the cycling of marine N_2O. The diagram is an adaptation of Figure 1 of *Capone* [1991].

as well as acting as a source. These reaction steps are also sensitive to local environmental conditions, most notably oxygen level. Denitrification has traditionally been viewed as a bacterial anaerobic respiration process; studies show that in the presence of oxygen, nitrate reduction ceases, and oxygen is preferentially consumed [*Ingraham*, 1981, *Bryan*, 1981].

Biological N_2O production from nitrification is believed to occur during the oxidation of ammonium to nitrite and nitrate. This process is mediated by a variety of nitrifying bacteria active in soils and natural water reservoirs [*Bremner and Blackmer*, 1981, *Ritchie and Nicholas*, 1972]. It has been suggested that two or more intermediates are produced during the oxidation of NH_4^+ to NO_2^-, the first of which is hydroxylamine (NH_2OH) [*Ritchie and Nicholas*, 1972]. N_2O is believed to be evolved during the oxidation of hydroxylamine to nitrite by the decomposition of, as yet, unidentified unstable intermediates; thus, in contrast to the denitrification process, N_2O is not a direct intermediary in the nitrification of ammonium to nitrate. As a result, the above sequence for N_2O production was not recognized as a potentially significant influence on the oceanic source until relatively recently [*Yoshinari*, 1976], although N_2O evolution during ammonium nitrification had been previously noted [*Yoshida and Alexander*, 1971, *Ritchie and Nicholas*, 1972]. In contrast to denitrification, the bacteria responsible for the majority of observed nitrification (e.g., Nitrobacter, Nitrosomonas) require oxygen for their activity, and nitrification is considered an aerobic process [*Bremner and Blackmer*, 1981]. The activity of nitrifying bacteria has also been demonstrated to display sensitivity to oxygen level, particularly at low O_2 concentrations [*Goreau et al.*, 1980, *Carlucci and McNally*, 1969]. Evolution of N_2O from nitrification is believed to constitute a very small fraction of the marine nitrogen cycle; that is, the magnitude of nitrogen involved in the oxidation pathway $NH_4^+ \rightarrow NO_2^-$ far outweighs that involved in the conversion of NH_4^+ to N_2O. *Butler et al.* [1987], having made a survey of oceanic measurements, report a range of 0.1-0.4% for the fraction of oceanic ammonium converted to N_2O in comparison to that converted to nitrite.

The process of assimilatory nitrate reduction, during which nitrate is reduced and incorporated into intracellular ammonium or aminonitrogen by organisms, is also believed capable of releasing N_2O as a by-product [*Delwiche*, 1981]. This reduction of nitrate to ammonium is most likely to be carried out by phytoplankton in the marine environment and has been suggested as an alternative source of N_2O in the surface ocean. The studies of *Hahn* [1981], *Pierotti and Rasmussen*, [1980] and *Oudot et al.* [1990] invoke this mechanism to account for very high surface N_2O levels in upwelling zones. There is, however, no direct support for such conclusions, and *Goreau et al.* [1980] found no evidence of N_2O release from cultures of phytoplankton; furthermore, *Cohen and Gordon* [1979] note that if such a source exists, it is probably of relatively small magnitude.

2.2. Oceanic Observations and Evolution of Views on N_2O Cycling

The prevalent view on the dominant mechanisms involved in the marine N_2O cycle has changed as information has accumulated on the variety of possible pathways involved in N_2O production and consumption. Early studies of surface oceanic N_2O encountered significant supersaturations in regions of the North Atlantic [e.g.,*Hahn*, 1974], and raised the possibility that the ocean provided a large biologically produced source of N_2O to the atmosphere. Since N_2O was known to be an intermediate product in the denitrification of nitrate to gaseous nitrogen, and denitrification was already established as an important source of N_2O in soils, studies in the 1970s proposed that this mechanism was responsible for the majority of marine N_2O formation [*Junge and Hahn*, 1971, *Hahn*, 1974].

Later measurements of subsurface N_2O, made in conjunction with observations of other oceanic properties, indicated negative correlations with the local oxygen distribution [*Yoshinari*, 1976, *Cohen and Gordon*, 1978]. Figure 2 depicts a range of reported observations of the vertical profiles of subsurface N_2O and oxygen. As can be seen, the deep N_2O distribution is a mirror image of oxygen, increasing with depth from the surface to a maximum in the vicinity of the oxygen minimum. Positive linear correlations between "excess N_2O" (defined as $\Delta N_2O = [N_2O]_{measured} - [N_2O]_{saturation}$) and apparent oxygen utilization (AOU) were first reported by *Yoshinari* [1973] and subsequently observed by other studies, including *Cohen and Gordon* [1979], *Elkins et al.* [1978], *Butler et al.* [1989], and *Oudot et al.* [1990]. These findings, among others, are summarized in Table 1 and plotted in Figure 3. In addition, the subsurface N_2O profiles were found to bear a close relation to the local nitrate distributions [*Cohen and Gordon*, 1979, *Butler et al.*, 1989, *Yoshida et al.*, 1989, *Oudot et al.*, 1990]. These characteristics of the N_2O distribution have been interpreted as suggesting a mechanism of N_2O production (most likely during nitrification) accompanying oxygen consumption and nutrient regeneration during organic matter remineralization in deep water [*Yoshinari*,1973; *Cohen and Gordon*,1978,1979; *Elkins et al.*,1978].

As can be seen from Figure 3, the observed linear relationships between ΔN_2O and AOU in different marine environments display a variety of slopes and intercepts. Postulated reasons for these differences include mixing of water masses, spatial variations in the abundances

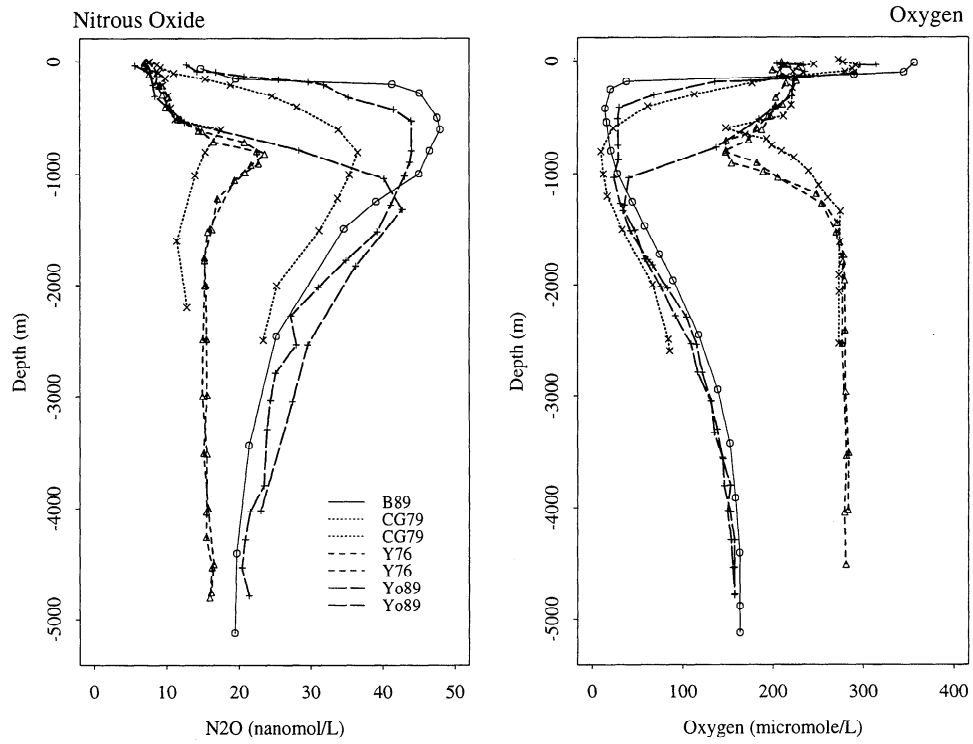

Figure 2. Observed depth profiles of deep N_2O and oxygen at a range of sites. The N_2O distribution is seen to be a mirror image of the oxygen distribution and displays a marked maximum in the region of the oxygen minimum. The data are taken from the following studies: *Butler et al.* [1989] (B89), *Cohen and Gordon* [1979] (CG79), *Yoshinari* [1976] (Y76), *Yoshida et al.* [1989] (Yo89).

of nitrifying organisms, variations in availability and composition of oxidizable organic matter, and influences from other localized sources and sinks of N_2O [*Cohen and Gordon*, 1978, *Elkins et al.*, 1978]. The observed relationships between N_2O and the oxygen distribution (and between ΔN_2O and AOU) are seen to break down in anoxic environments. In these regions, the characteristic N_2O maximum at the depth of the oxygen minimum disappears; instead, N_2O concentrations drop to very low levels. It is believed that the dominant influence on N_2O, in such environments, is the consumption of the gas by denitrifying bacteria that metabolize N_2O as a source of oxygen for respiration [*Elkins et al.*, 1978, *Cohen and Gordon*, 1978, *Hashimoto et al.*, 1983].

In view of the above evidence, the prevalent view established during the 1980s, and widely accepted today, is that N_2O is formed by nitrification processes in oxygenated water and consumed by denitrification in anoxic zones. However, this view is not universal and some studies still uphold denitrification as the primary pathway for N_2O formation [e.g., *Yoshida et al.*, 1989]. It is difficult to reconcile the high levels of N_2O observed in the well-oxygenated waters of the open ocean with a formation mechanism of denitrification, which is known to be inhibited by even very low O_2 levels; it has therefore been speculated by *Yoshida et al.*[1989], among others, that water column N_2O production from denitrification may occur in anaerobic microsites (e.g., the interiors of organic particulate matter or inside zooplankton guts). In addition, evidence has also accumulated over the recent years on a variety of potential influences on the mechanisms of marine N_2O formation; evidence that considerably complicates the relatively simple scenario of the oceanic N_2O cycle presented above. These complexities and alternative hypotheses on N_2O formation are discussed in section 2.3.

2.3. Complexities and alternative hypotheses

The mechanisms of marine N_2O production and consumption are known to exhibit significant complexity at low oxygen levels. As discussed previously, N_2O is often depleted in anoxic waters, a characteristic frequently attributed to consumption by denitrifying bacteria. Furthermore, elevated levels of N_2O are observed in suboxic waters and at the peripheries of anoxic zones [*Codispoti et al.*, 1989, *Ward et al.*, 1989, *Codispoti and Christensen*, 1985] suggesting enhanced N_2O production in these regions. Laboratory studies of nitrifying and denitrifying bacteria also demonstrate complex behavior and increased N_2O yields under low oxygen

Table 1. Observations of ΔN_2O versus AOU Relationships in Different Marine Environments.

Study	Location	Depth (m)	Regression Equation $\Delta N_2O = a\ AOU + b$ Slope a (nmol/μmol)	Intercept b (nmol)	Comments
Cohen and Gordon [1979]	NW Atlantic	100-2500	0.089(±0.003)	-0.437	Four stations reported by *Yoshinari* [1973]
	NE Pacific	0-800	0.076(±0.003)	-0.928	Data from *Cohen et al.* [1977]
	NE Pacific	1000-2500	0.218(±0.026)	-46.248	
	ETN Pacific	0-125	0.140(±0.0.004)	0.909	Only samples with $O_2 > 17$ μmol L^{-1}
Oudot et al. [1990]	ET Atlantic	0-250	0.129(±0.003)	2.1	
	ET Atlantic	0-20/40-70	0.219(±0.004)	2.2	
		0-20/150-250	0.160(±0.003)	1.96	
		0-20/50-250	0.162(±0.003)	2.3	
Hahn [1981]	N Atlantic	Above deep N_2O maximum	0.102	0.072	
		Below deep N_2O maximum	0.185	-0.135	
Law and Owens [1990]	Arabian Sea		0.31	-49.4	AOU > 197 μmol L^{-1}
			0.033	5.5	AOU < 197 μmol L^{-1}
Naqvi and Noronha [1991]	Arabian Sea	0-1000	0.17	(5)	Intercepts not reported; value listed is estimated from Figure 5
Butler et al. [1989]	W Pacific		0.125 + 0.00993T	-13.5	Regression equation includes dependance on temperature T
Elkins et al. [1978]	Eq. Pacific		0.0916 + 0.014T	-4.86	Regression equation includes dependance on temperature T

Abbreviations : NW (North West), NE (North East), ET (Eastern Tropical), ETN (Eastern Tropical North), Eq. (Equatorial).

conditions [*Carlucci and McNally*, 1969, *Goreau et al.*, 1980, *Jorgensen et al.*, 1984]. The mechanisms responsible for such behavior have not, as yet, been identified. Studies have postulated processes of enhanced nitrification [*Codispoti et al.*,1989,1992], as well as alternative mechanisms such as a complex coupling of nitrification and denitrification reactions at very low oxygen levels [*Codispoti and Christensen*, 1985, *Law and Owens*, 1990]. Recent studies of marine nitrous oxide have focused attention on the biologically productive regions associated with ocean basin eastern boundaries and characterized by regions of upwelling overlying oxygen deficient environments. The extremely high N_2O levels observed in these regions, and the com-

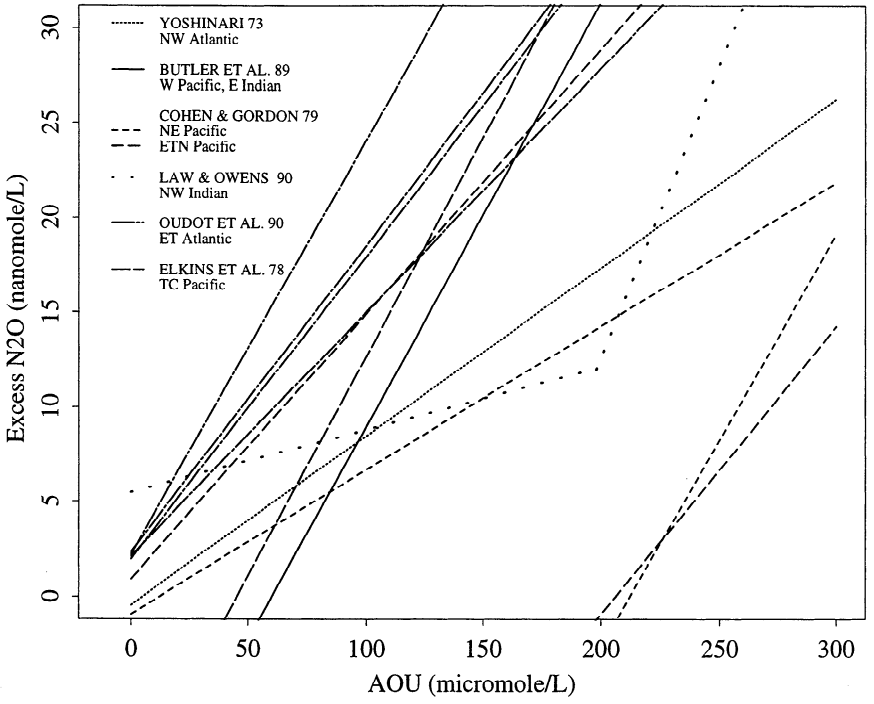

Figure 3. Reported relationships between deep ΔN_2O and AOU. Studies depicted and corresponding oceanic regions are the following: *Yoshinari* [1973], northwest Atlantic; *Butler et al.* [1989], west Pacific and east Indian; *Cohen and Gordon* [1979], northeast Pacific and eastern tropical north Pacific; *Law and Owens* [1990], northwest Indian; *Oudot et al.* [1990], eastern tropical Atlantic; *Elkins et al.* [1978], tropical central Pacific. The correlations for the temperature dependent relationships of *Elkins et al.* [1978] and *Butler et al.* [1989] are plotted for a temperature of 10°C.

plex nature of the N_2O cycling processes associated with these suboxic zones, have given rise to speculation that such regions may contribute a significant fraction of the ocean-atmosphere N_2O flux [*Codispoti et al.*, 1992, *Law and Owens*, 1990, *Codispoti and Christensen*, 1985], and also may be responsible for some proportion of the larger-scale N_2O distribution in the oceanic interior [*Codispoti et al.*, 1992, *Codispoti and Christensen*, 1985]. (The issues raised by these studies are further explored by *Suntharalingam* [1997] and *Suntharalingam et al.* [2000].

Wahlen and Yoshinari [1985] noted that analysis of the isotopic signatures of N_2O from a variety of environments offered a promising means of identifying the primary formation pathways. Since the fractionation effects associated with nitrification and denitrification have different signatures, evaluation of observed isotopic ratios in marine N_2O should enable a disentangling of the respective effects. Rather than clarifying the various N_2O cycling processes, however, the isotopic measurements have led to controversy, as they have been subject to a variety of interpretations, frequently contradictory. *Yoshida et al.* [1989] have invoked the deep ^{15}N enrichment observations to support a dominant production mechanism of denitrification. *Kim and Craig* [1990] use the same data to suggest that the majority of oceanic N_2O is formed by nitrification; *Naqvi* [1991] and *Naqvi et al.* [1998] interpret the $\delta^{15}N$ occanic signatures as demonstrating N_2O production through a coupling of nitrification and denitrification with NO as an intermediary. At this stage, the issues still remain somewhat unresolved, and further work is obviously necessary.

The studies of *Elkins et al.* [1978] and *Butler et al.* [1989] noted that deep ΔN_2O/AOU ratios displayed a linear positive correlation with temperature and speculated that N_2O production is influenced by local temperature. This suggestion of a temperature dependence in the N_2O formation process is lent support by the laboratory work of *Yoshida and Alexander* [1970] who demonstrated a temperature sensitivity in activities of nitrifying bacteria. The deepwater data of *Butler et al.* [1989] also indicate a negative correlation between local pressure and N_2O concentration at depths below 1500 m; the authors attribute this observed effect to preferential production of ionic nitrate, rather than gaseous N_2O, from ammonium oxidation at high pressures. It does not seem likely, however, that this reaction will have a significant impact on oceanic N_2O cycling, as the majority of organic matter remineralization occurs

well above 1000 m [*Najjar et al.*, 1992, *Anderson and Sarmiento*, 1995].

The previously discussed mechanisms of marine N_2O cycling are predominantly concerned with water column processes, and the majority of the measurements discussed were made in the open ocean. A laboratory study by *Jorgensen et al.* [1984], on N_2O formation in marine sediments, indicates enhanced levels of N_2O production from both nitrification and denitrification processes as the local oxygen concentration drops to suboxic levels. The authors suggest that this effect may be important in coastal sediments but do not indicate whether the N_2O thus formed undergoes further denitrification to N_2, or speculate on the relative magnitudes of sedimentary N_2O yield in comparison to global water column N_2O production. Studies in estuarine and coastal regions have measured N_2O fluxes from shallow sediments [*Jensen et al.*, 1984, *Seitzinger et al.*, 1984], and these fluxes have been attributed to both nitrifying and denitrifying activity [*Capone*, 1991]. The magnitude of net N_2O fluxes from sediments has not traditionally been considered significant, and thus usually neglected in an accounting of oceanic N_2O production. A recent study by *Capone* [1991] suggests, however, that fluxes from the sediments (predominantly in coastal areas) could account for over 40% of the net oceanic production.

As has been outlined above, current understanding of the processes governing the production and distribution of marine N_2O is far from complete. In this study we have focused not on the specific complexities detailed above but on the widely accepted current interpretation of the ΔN_2O and AOU data as suggesting a dominant pathway for N_2O formation during organic matter oxidation in the aphotic zone. Details of the model components and configuration are presented in section 3.

3. Model Description

The modeling analysis simulates N_2O as a nonconserved tracer in an ocean general circulation model (OGCM); N_2O is subject to physical transport via the ocean dynamics, biological source and sink mechanisms, and gas exchange at the ocean surface. The basis for the model of the oceanic N_2O source is provided by the observed correlations between ΔN_2O and AOU and the associated interpretation of N_2O production accompanying oxygen consumption during the remineralization of organic matter below the euphotic zone. In addition to a 3-D circulation model therefore, we also employ a model of N_2O formation linked to an organic matter cycling model, as well as a representation of gas exchange to provide the necessary boundary condition at the ocean surface.

A simple schematic diagram of the N_2O model and its relationship to each of the other modeling components is presented in Figure 4. Briefly, organic matter formed in the euphotic zone by photosynthesis is transported into the deeper aphotic zone, where, under biological action, it is remineralized into its inorganic constituents. N_2O is evolved as a by-product during this process; the production of N_2O is keyed to the amount of oxygen consumption taking place during remineralization. The choice of relationship governing N_2O production to oxygen consumption is further discussed in section 3.3. The resulting N_2O is transported within the deep ocean and into the surface euphotic zone by the oceanic circulation. Once at the surface, it is free to exchange with the atmosphere across the air-sea interface. Sections 3.1 - 3.4 describe each of the model components in more detail.

3.1. Ocean Circulation Model

The circulation model used for all the simulations in this study is the Modular Ocean Model (MOM) [*Pacanowski et al.*, 1993] developed at the Geophysical Fluid Dynamics Laboratory (GFDL). It is based on the primitive equation numerical model of *Bryan and Cox* [1967]. The configuration employed in this analysis is a modified version of the prognostic model (Model P) of *Toggweiler et al.*[1989a,b]. It has been described extensively in these latter studies, therefore we limit the discussion here to a brief summary.

The model is a nonseasonal global ocean GCM of horizontal resolution 4.5° latitude by 3.75° longitude, has 12 levels in the vertical and has a maximum depth of 5000 m. Mixing by subgrid scale processes is parameterized by horizontal and vertical diffusion coefficients A_{HH} and A_{HV}. For this configuration of the model A_{HH} ranges from 1.0×10^7 cm^2 s^{-1} at the surface to 0.5×10^7 cm^2 s^{-1} at depth. The vertical diffusion coefficient, A_{HV}, increases from 0.3 cm^2 s^{-1} in the surface ocean to 1.3 cm^2 s^{-1} at depth.

The model is forced at the surface by the annual mean wind stresses of *Hellerman and Rosenstein* [1983], and surface forcing heat and freshwater fluxes are calculated by restoring model potential temperature and salinity to the annual climatological averages of *Levitus et al.* [1982]. Modifications to the prognostic model of *Toggweiler et al.* [1989a] incorporated in the current version are described by *Toggweiler and Samuels* [1993] and include the closing of the Indonesian Straits and the lengthening of the surface salinity restoring timescale to 120 days.

3.2. Ocean Biogeochemistry Model

The Ocean Biogeochemistry Model (OBM) simulates oceanic new production and remineralization and consists of tracers for the nutrient and oxygen cycles em-

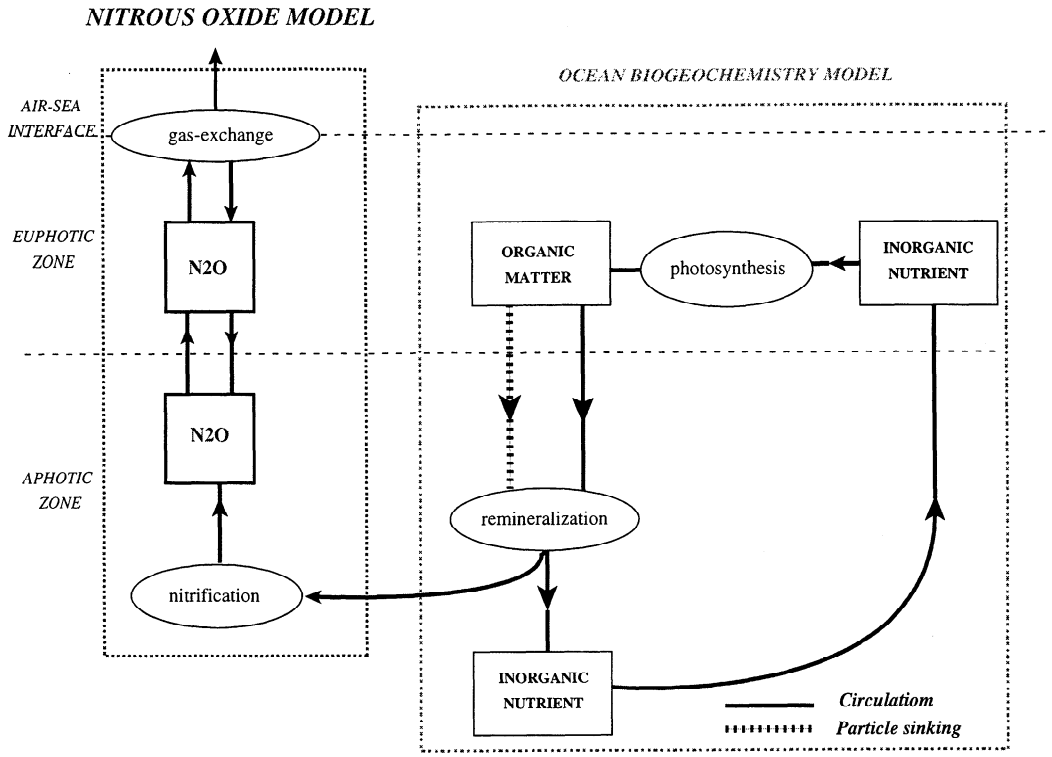

Figure 4. Schematic representation of the relationship of the N_2O source model to the other model components, i.e., ocean circulation model, Ocean Biogeochemistry Model, and gas exchange).

bedded in the OGCM [*Sarmiento et al.*, 1995, *Murnane et al.*, 1999]. The organic matter cycle is based on phosphate and draws on the work of *Najjar* [1990], *Najjar et al.* [1992] and *Anderson and Sarmiento* [1995]. The modeled tracers relevant to this study include dissolved organic phosphorus (DOP), phosphate, and oxygen. These tracers are transported by the advection, diffusion, and convection fields of the OGCM. There is, in addition, a pool of particulate organic phosphorus (POP) which is transported only by vertical sinking.

New production of organic matter occurs in the euphotic zone (the first two levels of the model, of maximum depth 119 m), by restoring phosphate levels to observations from *Najjar et al.* [1992] on a 100 day timescale. This production is partitioned into dissolved and particulate organic matter; the partition fraction is taken to be 0.5, as recommended by *Anderson and Sarmiento* [1995]. The POP is immediately transferred out of the euphotic zone and remineralizes directly below its location of formation. The flux of POP at a depth z is parameterized using the sediment trap observations of *Martin et al.* [1987]; the remineralization profile is given by the rate of change of this flux with depth. DOP is transported by the OGCM circulation, and remineralizes at a rate proportional to its local concentration. This net export of organic matter from the euphotic zone which remineralizes in the aphotic zone is responsible for driving oxygen consumption and the modeled N_2O source.

3.3. N_2O Model

The tracer equation for the local concentration of N_2O is

$$\frac{d}{dt}[N_2O] = \frac{\partial}{\partial t}[N_2O] + \mathbf{V}\cdot\nabla_H[N_2O] + w\frac{\partial}{\partial z}[N_2O]$$
$$= A_{IIH}\nabla^2[N_2O] + \frac{\partial}{\partial z}\left(A_{HV}\frac{\partial}{\partial z}[N_2O]\right) + J_{N_2O} \quad (1)$$

J_{N_2O} represents the source minus sink terms for N_2O. On the basis of the observed correlations between ΔN_2O and AOU, N_2O simulations considered in this study model a nitrous oxide source as a function of local oxygen consumption (accompanying organic matter remineralization) in the aphotic zone, thus,

$$J_{N_2O} = f[O_{2\ \text{consumption}}] \quad (2)$$

We discuss the Base Case formulation for J_{N_2O} here. The standard simulation, or Base Case, assumes a simple linear proportionality between the two quantities (based on the linear relationships seen between ΔN_2O and AOU in the observational studies). Thus

$$J_{N_2O} = \alpha \times [O_2 \text{ consumption}] \qquad z \leq z_e \qquad (3)$$

where z_e represents the depth of the euphotic zone, and z is taken as positive upward. The molar ratio selected for α for the Base Case simulation is

$$\alpha = 0.1 \times 10^{-3} \quad \frac{\text{mol}\,N_2O}{\text{mol}\,O_2} \qquad (4)$$

This value represents a "low average" of the reported ratios; its relationship to the observations is depicted in Figure 5. *Elkins et al.* [1978], in a study of N_2O in the Central Pacific, noted that the magnitude of the ΔN_2O/AOU correlations was about twice as large for measurements made in "active" regions of upwelling and biological productivity, in contrast to measurements outside these regions. The Base Case value for α is therefore motivated by the fact that several of the measurement sites included in Table 1 are located in regions of higher productivity; thus a simple average may be biased toward higher ΔN_2O/AOU ratios and therefore not representative of a global average. Since this selection of α is somewhat arbitrary, we have also conducted a set of sensitivity tests to reflect the range of the observed values for the ΔN_2O/AOU correlations; i.e., for α varying from 0.07×10^{-3} [*Cohen and Gordon*, 1979] to 0.22×10^{-3} [*Oudot et al.*, 1990]. These scenarios will be discussed briefly in this study and are presented in more detail by *Suntharalingam* [1997].

Nitrate regeneration from ammonium oxidation, has been considered unimportant in the euphotic zone, as nitrifying bacteria are believed to be inhibited by light [*Horrigan et al.*, 1981]. N_2O production from nitrification processes in the euphotic zone is also therefore assumed to be insignificant. Additional sources of N_2O resulting from processes such as assimilatory nitrate reduction in the euphotic zone are believed to be relatively small [*Cohen and Gordon*, 1978]. Furthermore, observations made by *Cline et al.* [1987] in the euphotic zone of the eastern equatorial Pacific suggest that N_2O can be considered quasi-conservative at these depths. Therefore, in all the simulations considered in this study, N_2O production is only assumed to occur in the aphotic zone. Thus, in the euphotic zone,

$$J_{N_2O} = 0 \qquad z \geq z_e \qquad (5)$$

N_2O is exchanged with the atmosphere across the air-sea interface using a parameterized gas exchange process as discussed in section 3.4.

3.4. Gas Exchange

The flux of N_2O across the air-sea interface is calculated as a product of the gas-transfer velocity k_w and the concentration difference across the interface, thus

$$F_{N_2O} = (1 - f_i)k_w([N_2O]_{atm} - [N_2O]_{ocean}) \qquad (6)$$

where f_i represents the fraction of the local ocean sur-

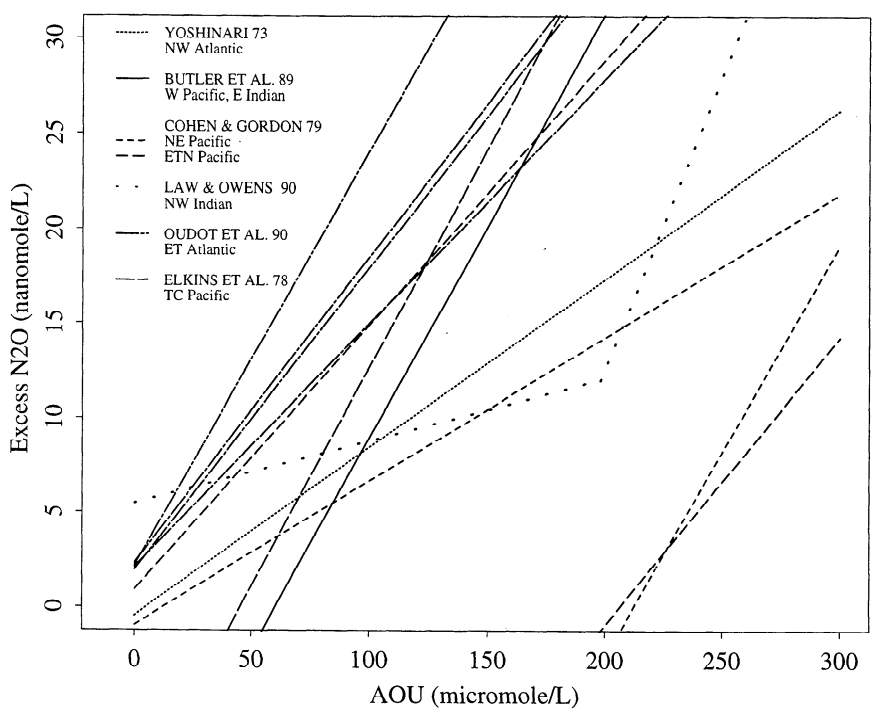

Figure 5. N_2O source parameterization chosen for Base Case Model in comparison to the observed ΔN_2O versus AOU correlations. The molar ratio governing N_2O production to oxygen consumption is $\alpha = 0.1 \times 10^{-3}$.

face under icecover. k_w, the gas-transfer velocity, is influenced in a complex manner by interfacial turbulence, the kinematic viscosity of the water μ, and the diffusion coefficient of the gas D. It is often parameterized as a function of wind speed U, and the Schmidt number Sc, which represents the dependence of k_w on the latter two terms (i.e., $Sc = \mu/D$). The gas-transfer velocity employed for the simulations in this study is the formulation of *Wanninkhof* [1992],

$$k_w(U, Sc) = 0.39U^2(\frac{Sc}{660})^{-0.5} \quad (7)$$

Wanninkhof's [1992] formulation for long-term, as opposed to steady, winds is used, in keeping with the climatologically averaged wind speed data set used for the simulations [*Esbensen and Kushnir*, 1981]. Since we aim to examine the steady state oceanic N_2O distribution and not transients due to atmospheric N_2O increase, the atmospheric partial pressure of N_2O is fixed at the preindustrial level of 285 natm; we employ solubility parameterizations from *Weiss and Price* [1980] for conversion to the oceanic saturation concentration $[N_2O]_{atm}$.

Parameterization of the gas-exchange coefficient for application on large regional and global scales is still subject to a considerable degree of uncertainty. Estimates derived from methods calibrated by oceanic uptake of radiocarbon [e.g., *Wanninkhof*, 1992] differ by a factor of 2 from those based only on tracer release experiments in lakes and wind-wave tanks [e.g., *Liss and Merlivat*, 1986]. While the net global sea-air N_2O flux in the simulations of this study is determined directly by the model biological parameterizations, variation in the representation of gas exchange does have a small effect on modeled concentrations near the ocean surface in upwelling zones and in regions of rapid vertical mixing. This effect has been explored by *Suntharalingam and Sarmiento* [1995] and *Suntharalingam* [1997] by contrasting the effects of the *Wanninkhof* [1992] parameterization against that of *Liss and Merlivat* [1986]. Use of the *Wanninkhof* [1992] formulation for gasexchange was found to yield surface concentrations that better matched the magnitude of observational data for N_2O.

4. Base Case Simulations

This section focuses on evaluation of the simple Base Case parameterization for the N_2O source as described in section 3.3. Modeled surface fluxes and the oceanic interior N_2O distribution are compared with observational results derived from the surface oceanic N_2O data of *Weiss et al.* [1992] and the deepwater data of *Butler et al.* [1988].

4.1. Surface Distributions and Fluxes

Observational evidence suggests that high N_2O surface supersaturations are observed in biologically productive upwelling regions, with values closer to equilibrium and small undersaturation in the oceanic gyres [*Butler et al.*, 1989, *Weiss et al.*, 1992]. Plate 1 presents a map of modeled surface ΔpN_2O; for comparison we also present in Plate 2 a map based on the observations of *Weiss et al.* [1992]. (The derivation of the observational distribution from the data of *Weiss et al.* [1992] is based on multivariate regression relationships between surface N_2O and local biological and physical variables; the methodology is discussed in detail by *Suntharalingam* [1997].) Comparison of the modeled and observational surface distributions for ΔpN_2O indicates that the model is successful in reproducing the characteristic features of the large-scale distribution. High values, in excess of 60 natm, are seen in the equatorial and coastal upwelling regions, and undersaturation and values close to equilibrium are obtained in the subtropical gyres. Also obvious in Plate 1, however, are certain localized high N_2O features in the southern high latitudes (at approximately 40°-50°S). These are not present in the observational map and are most likely unrealistic; these features are caused by characteristics of the circulation model and will be discussed later in this section.

Figure 6 depicts the zonally integrated flux from the Base Case model and compares the sea-air flux derived from different latitudinal bands with the data based estimates from *Nevison et al.* [1995] (N95) and *Suntharalingam* [1997] (S97). (Both these observational estimates rely primarily on the *Weiss et al.* [1992] database for measurements of ΔpN_2O. Methods of interpolation, however, differ between the two studies and are discussed by *Suntharalingam* [1997].) As can be seen, the observations suggest an approximately trimodal zonal flux distribution with maxima in the tropics and in the high northern and southern latitudes (centered at 50°N and 50°S). The modeled distribution matches this trimodal pattern, with significant maxima in the southern high latitudes and equatorial regions and a somewhat less pronounced maximum in the northern high latitudes. The minima of the meridional flux distribution are centered in the subtropical gyres at 30°S and 30°N. Despite the similarity in structure between the modeled and observed flux distributions, the model results predict the highest fluxes in the 90°-30°S band, in comparison to the observational predictions of maximum fluxes in the 30°S-30°N band. In addition, other local differences are evident between modeled and observed flux distributions. Many of these discrepancies, as well as disparities between the modeled and observed surface ΔpN_2O distributions, can be traced to characteristics of the circulation model and are discussed in turn below.

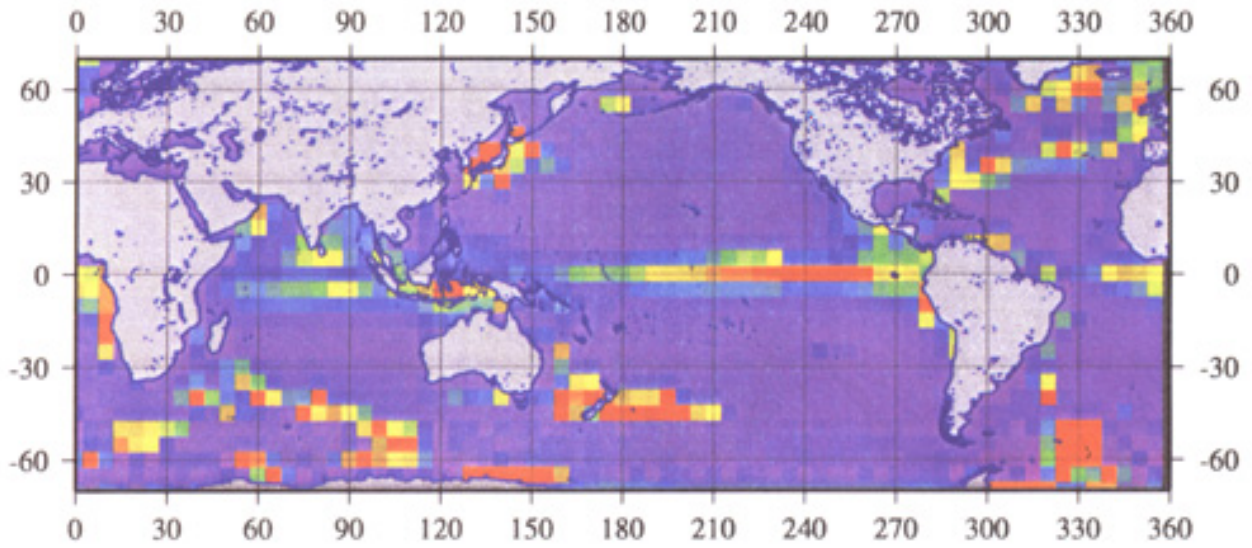

Plate 1. ΔpN_2O (natm) surface field obtained for the Base Case simulation.

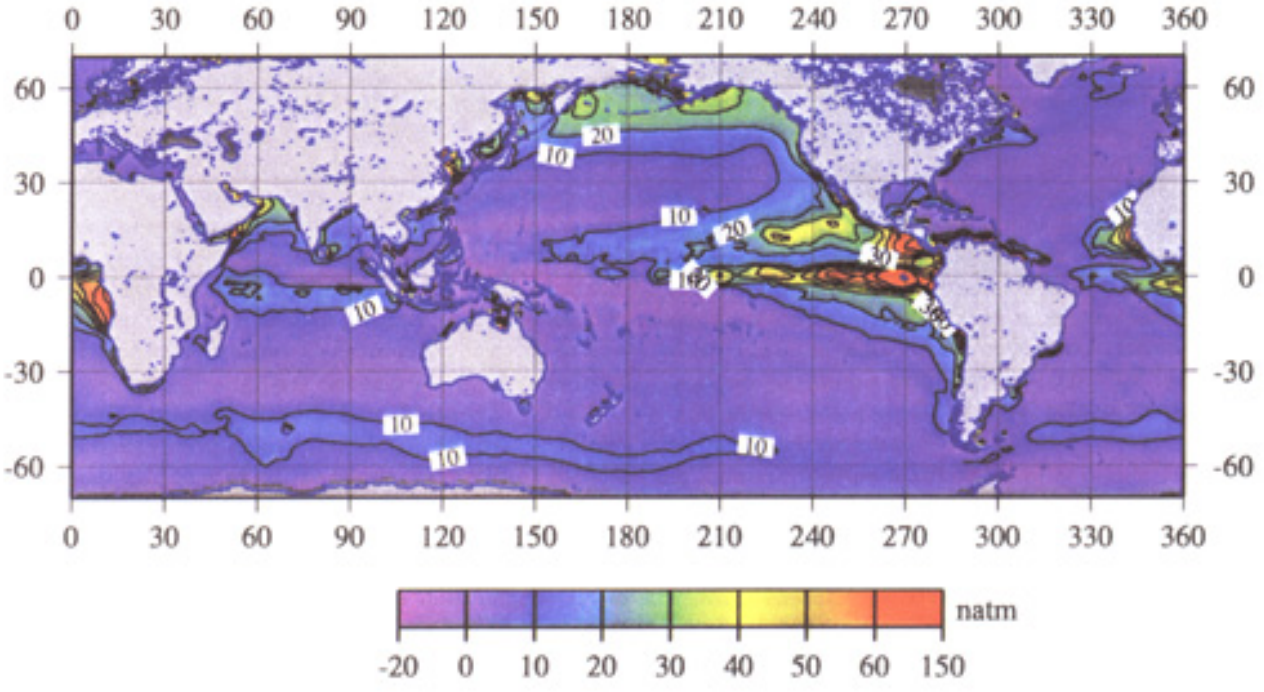

Plate 2. ΔpN_2O (natm) surface field derived from the *Weiss et al.* [1992] database. The data were binned to a $1^\circ \times 1^\circ$ resolution and extrapolated according to the method discussed in *Suntharalingam* [1997].

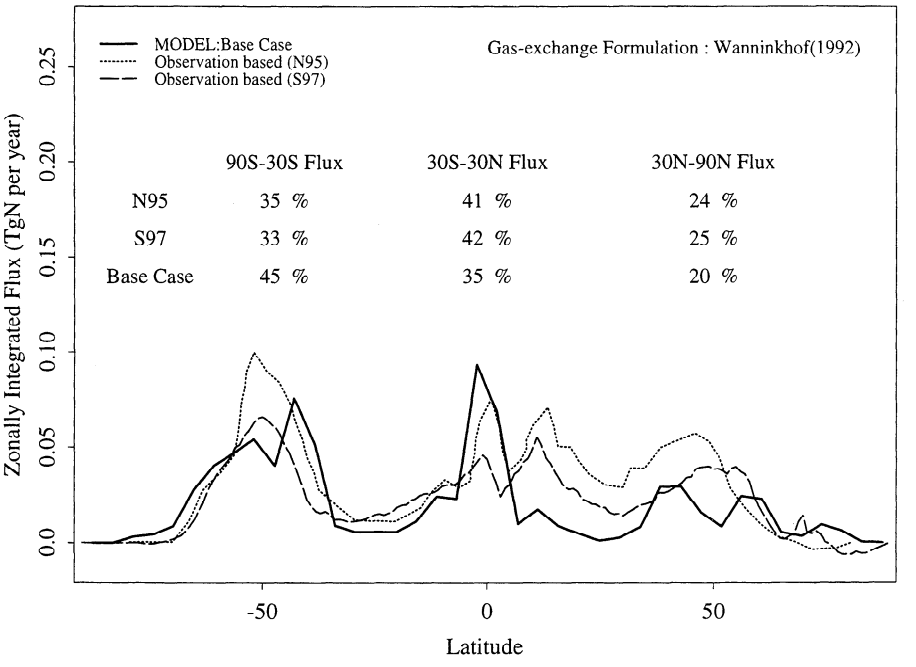

Figure 6. Zonally integrated flux from the Base Case model and comparison with observation based estimates of *Nevison et al.* [1995] (N95) and *Suntharalingam* [1997] (S97). The observational estimates both rely primarily on the *Weiss et al.* [1992] database for ΔpN_2O.

4.1.1. Southern Ocean. Particularly apparent in Plate 1 are localized features of high surface N_2O in the southern high latitudes that have no counterparts in the observation-based map. The observational database of *Weiss et al.* [1992] is sparse in these regions; however, since the OGCM is acknowledged to produce certain anomalous convective features in these latitudes [*Toggweiler et al.*, 1989a], it is likely that these features are modeling artifacts. Figure 7 depicts the locations of highest convective frequency in the upper 400 m of the OGCM. A comparison of Figure 7 with Plate 1 indicates a close correlation between the locations of high ΔpN_2O levels in the Southern Ocean and the zones of intense convection at these latitudes. The locations and intensities of these convective zones are most likely unrealistic; however, they do have significant implications for the modeled N_2O distribution and sea-air flux. First, they act as a conduit for mixing up deeper water with high N_2O concentrations to the surface. Second, as was noted by *Najjar* [1990], these regions display very high localized new production levels due to the following mechanism; organic particulate matter remineralizes into nutrients at depth, and these nutrients are then mixed back up to the surface in these regions with the very short timescales characterizing intense convection (e.g., zonally averaged new production levels at some latitudes in the Southern Ocean exceed 7 mol C m^{-2} yr^{-1} which, in contrast to the primary production values of 5-8 mol C m^{-2} yr^{-1} suggested for these regions by *Berger* [1989], indicates that local levels of modeled new production values are far too high). The resulting high remineralization rates and concomittant oxygen consumption directly affect N_2O production; thus these regions also act as high N_2O source locations.

As noted previously, there is a disparity between model and observational estimates of the latitudinal zones of maximum N_2O efflux. The Base Case scenario predicts the highest proportion of the sea-air flux (45%) in the southern high latitudes (90°-30°S), while the observations predict highest fluxes from the tropical latitudes (30°S-30°N). An important cause of this disparity in the Southern Ocean is most likely due to localized model overestimates of new production and remineralization resulting in high N_2O production, as well as intensification of N_2O vertical transport in the anomalous convective zones.

4.1.2. Tropical and North Pacific. Figure 6 indicates that the zonally integrated observational flux pattern displays two peaks in the tropical regions, one linked to the zone of equatorial upwelling and another at approximately 5°N. As seen in Plate 2 of the observation-based ΔpN_2O field, the source of this second peak is primarily the high supersaturation in the north east tropical Pacific (NETP). Observational evidence indicates that the anoxic and suboxic regions in the eastern Pacific, namely, the NETP off the coast of Central America, and the upwelling region off Peru, are sites of high N_2O production and turnover; surface supersaturations in excess of 70% have been measured [*Weiss et al.*, 1992] indicating potentially important sites of

N_2O efflux [*Codispoti and Christensen*, 1985, *Codispoti et al.*, 1989]. The high N_2O levels in these regions are associated with the local coastal upwelling and high productivity; furthermore, studies have suggested that complex N_2O cycling mechanisms at low oxygen levels could result in enhanced N_2O production in the suboxic regions characteristic of the eastern tropical Pacific [*Codispoti et al.*, 1992, *Codispoti and Christensen*, 1985]. The simple source parameterization of the Base Case (linked solely to productivity) does not allow for sensitivity to factors such as local oxygen level. In the tropical Pacific therefore the Base Case model produces the highest levels of surface N_2O at the equator in the center of the basin in conjunction with the location of highest upwelling [*Toggweiler et al.*, 1989a]. Thus the two distinct high N_2O regions observed off the coast in the Eastern Tropical Pacific are not well delineated. Modeled tropical fluxes are influenced by this high equatorial N_2O zone which results in the dominance of the equatorial flux maximum seen in Figure 6 rather than in the two distinct maxima seen in the observed distributions.

Comparison of modeled surface ΔpN_2O in the North Pacific (Plate 1) with the observationally derived distribution (Plate 2) indicates that the model values are close to equilibrium with the atmosphere and do not reproduce the higher supersaturations seen in the observational distribution. Our analysis of the observational data by *Suntharalingam* [1997] indicates that the elevated ΔpN_2O values in the North Pacific are linked to enhanced local productivity. The disparity between model and observational flux estimates in these latitudes could, therefore, be a consequence of model underestimates of local productivity and remineralization and hence of N_2O formation in these latitudes. The study of *Anderson and Sarmiento* [1995] which also employed this ocean biogeochemistry model noted that new production and oxygen consumption are underestimated in the northern high latitudes (specifically at 50°N); possible causes cited include insufficient upwelling of nutrient, or overestimates of observed surface phosphate levels (which form the basis for the model's estimate of new production).

Our evaluation of the modeled surface N_2O field indicates indicates that the simple Base Case parameterization linking N_2O production to oxygen consumption is successful in reproducing the large scale features of the observed distribution; namely, high surface supersaturations in regions of upwelling and intense biological productivity, and saturation values close to equilibrium in the oligotrophic subtropical gyres. As itemized above, anomalous features of the surface N_2O distribution can be traced to characteristics of the circulation or ocean biogeochemistry model; for example, the lo-

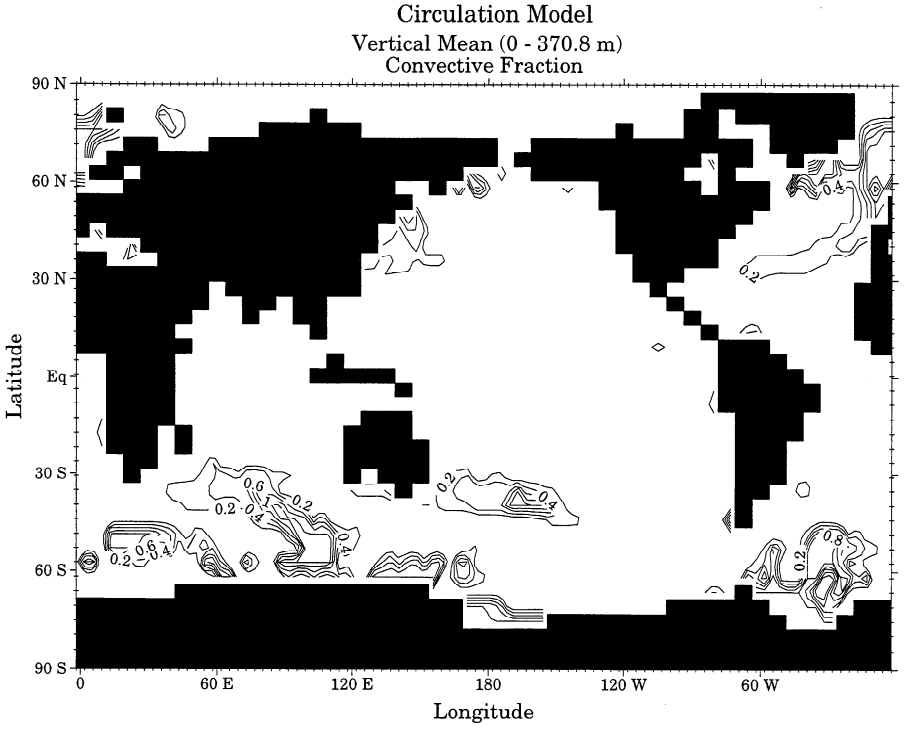

Figure 7. Regions of high convective frequency in the upper ocean of the circulation model (depth range of 0-370.8 m). The contour index indicates the fraction of the time the enclosed water column is undergoing convective adjustment; thus a value of 1 indicates continuous convective adjustment. The contour interval is 0.2.

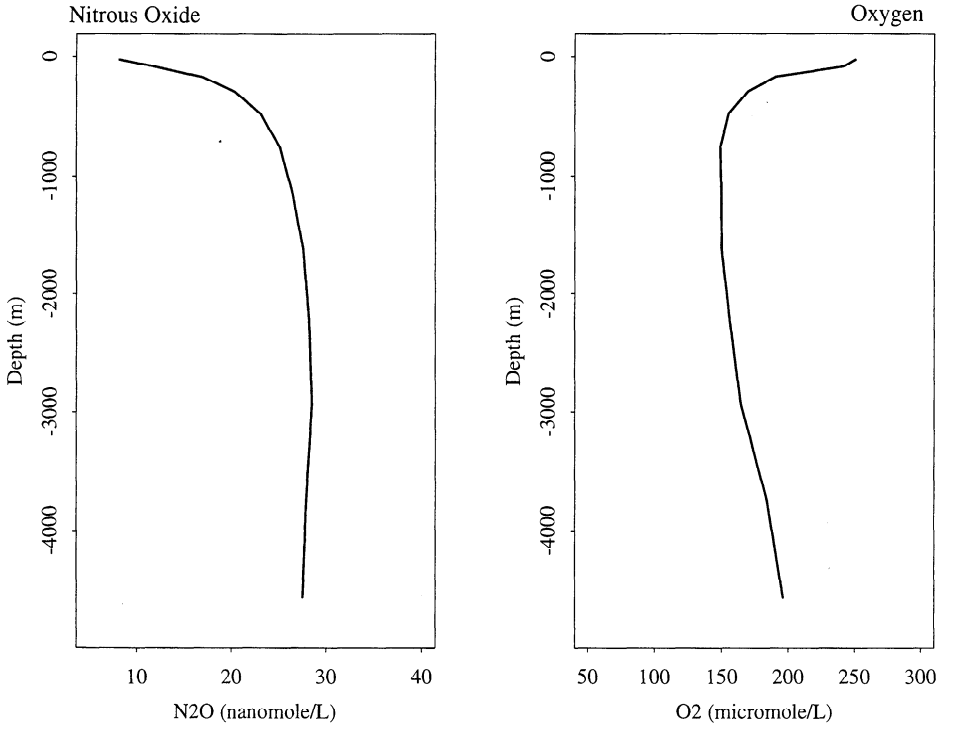

Figure 8. Globally averaged Base Case model depth profiles for N_2O and oxygen.

calized high N_2O regions in the southern high latitudes that result from the zones of intense deep convection in these regions. However, as will be discussed in section 4.2, this simple parameterization for N_2O production is not as successful in the deep ocean.

4.2. Distributions at Depth

Figure 8 depicts the globally averaged depth profiles for modeled nitrous oxide and oxygen; it can be seen that the modeled N_2O distribution displays an inverse relationship to the modeled O_2 distribution, increasing from levels of 6-10 nmol L^{-1} at the surface to a maximum of over 30 nmol L^{-1} at intermediate depths. Recall that the parameterization governing N_2O production in this Base Case simulation (i.e., $\alpha = 0.1$ [nmol N_2O production]/[μmol oxygen consumption]) was derived from the observed ΔN_2O/AOU correlations that displayed a range of values. Simulations were also conducted to examine the sensitivity of the modeled distributions and sea-air flux to α by varying its value to reflect the observed range in ΔN_2O/AOU correlations (i.e., from 0.07 (nmol ΔN_2O)/(μmol AOU) [*Cohen and Gordon*, 1979] to 0.22 (nmol ΔN_2O)/(μmol AOU) [*Oudot et al.*, 1990]); these results are discussed in detail by *Suntharalingam* [1997]. The main effect of a change in α is to scale the magnitude of the oceanic N_2O distribution and sea-air flux accordingly, with minor effects on the structure of the distribution (e.g., the proportional spatial distribution at the surface and at depth varies by less than 5%). This result is unsurprising, given the simplicity of the parameterized source function for N_2O. In view of the relative insensitivity of the structure of the oceanic N_2O distribution to the magnitude of α, this effect will not be further discussed here; in our evaluation of the success of the N_2O model we will focus only on the Base Case scenario.

As noted by *Najjar et al.* [1992] and *Anderson and Sarmiento* [1995], model simulations of dissolved gases such as nitrous oxide and oxygen in the upper ocean are sensitive to the warm thermocline characteristic of coarse grid OGCMs. *Najjar et al.* [1992] notes that the thermocline temperatures of the circulation model are up to 4°C warmer than the observations of *Levitus et al.* [1982]. A possible cause is that the thermocline is ventilated by waters formed at too low a latitude [*Toggweiler et al.*, 1989b]. A warmer than observed thermocline lowers the concentrations of dissolved gases such as nitrous oxide and oxygen whose solubility is a decreasing function of temperature. Thus a temperature difference of 4°C causes the levels of N_2O and oxygen in the thermocline to be lower than the observations by up to 2 nmol L^{-1} and 26 μmol L^{-1}, respectively. *Anderson and Sarmiento* [1995] note that in view of this 'warm thermocline' problem, it is more appropriate to examine AOU rather than the oxygen distribution, when evaluating biology models. AOU (defined as $[O_2]_{saturation}$ - $[O_2]_{measured}$) subtracts out the measured concentration from the local temperature depen-

dent saturation concentration, and enables evaluation of the predominantly biological contribution to oxygen levels. Similarly, when evaluating the success of the N_2O model simulations, we examine ΔN_2O (defined as $[N_2O]_{measured}$- $[N_2O]_{saturation}$).

Figure 9 depicts the Base Case ΔN_2O and AOU model results for the Pacific Basin and comparison with data from the SAGA II cruise reported by *Butler et al.* [1988]. This data set consists of 56 stations predominantly in the west Pacific and Indian Oceans. In evaluating the performance of the N_2O model at depth we have only compared the SAGA II data and the model results for the Pacific, since the portions of the Indian and Southern Ocean traversed by the SAGA II cruise include regions of known model anomalous circulation (e.g., the convective zones discussed in section 4.1). The modeled ΔN_2O values increase from the surface to a maximum of $\geq$ 20 nmol L^{-1} at intermediate depths of about 1500 m and then decrease slightly to a level of about 18 nmol L^{-1} in the deep ocean. This structure does not replicate very well the observed ΔN_2O profile of the *Butler et al.* [1988] data, which displays a pronounced maximum of up to 25 nmol L^{-1} at depths of 400-600 m, and a much steeper decline with depth dropping to less than 10 nmol L^{-1} in the deep ocean. Modeled deep ΔN_2O values are up to 10 nmol L^{-1} higher than the observations below depths of 3000 m. In contrast, the modeled AOU profile replicates the structure of the observed distributions, from *Levitus et al.* [1994] and *Butler et al.* [1988] much better; the modeled profile shows an increase with depth to a slight maximum between 1000-2000 m and subsequent gradual decrease with depth. It appears that while the depth structure of modeled AOU replicates the observations quite well, that of modeled ΔN_2O fails to do so with the same degree of success.

A comparison of the variation of modeled and observed ΔN_2O/AOU ratios with depth (Figure 10) indicates that the cause of the misfit between model and observations arises from the simplicity of the N_2O source parameterization. Recall that the Base Case parameterization was based on observed linear correlations between ΔN_2O and AOU; in modeling the oceanic N_2O source as a linear function of oxygen consumption, the parameter α relating the two was assumed to be constant everywhere in the global ocean. If, however, we examine the ΔN_2O/AOU ratios of the *Butler et al.* [1988] data as a function of depth along with the model results from the Base Case, as depicted in Figure 10, it is seen that the observational ΔN_2O/AOU ratios are not constant but display a systematic decrease with depth, ranging from 0.12×10^{-3} in the upper ocean

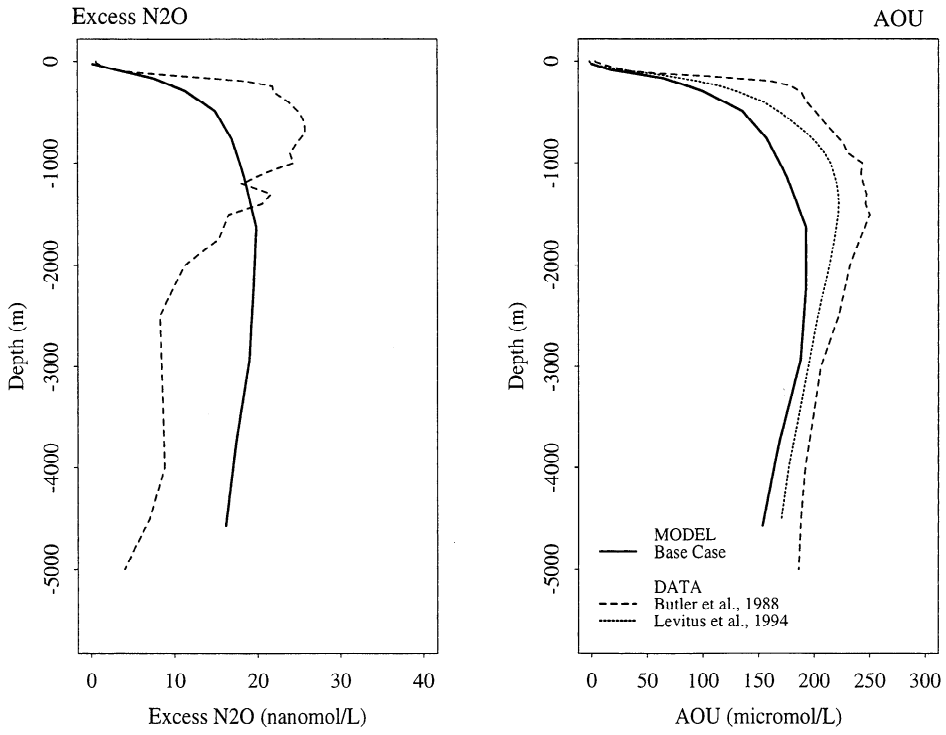

Figure 9. Profiles of excess N_2O (ΔN_2O) and AOU for the Base Case simulation and comparison with observations from *Butler et al.* [1988]. The comparison between model and observations has been made for values in the Pacific since the SAGA II cruise traversed regions of known model anomalous circulation in the Indian Ocean.

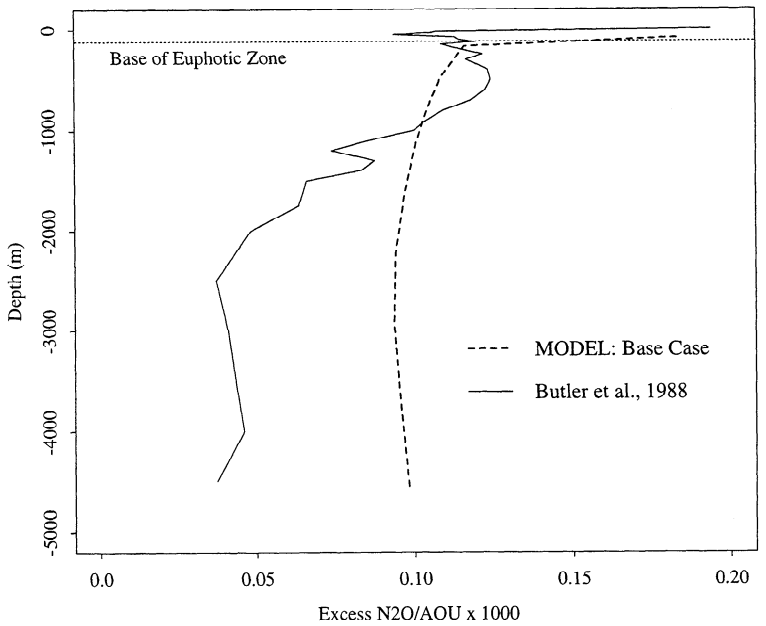

Figure 10. Variation of $\Delta N_2O/AOU$ ratio with depth for Base Case simulation and comparison with data from *Butler et al.* [1988].

to less than 0.05×10^{-3} below 4000 m. This depth decreasing feature of the observational data is not surprising, given the observation by *Butler et al.* [1989] (discussing the same database) that the $\Delta N_2O/AOU$ results varied with temperature. In most of the ocean, temperature can act as a proxy for some depth varying process. The parameterization of the Base Case, in comparison, fails to capture this aspect of the data. We therefore conclude that use of the SAGA II database as a constraint to validate the N_2O model suggests that the Base Case source function does not account for some, as yet unidentified, depth varying process in relating ΔN_2O and AOU; That is, a much lower ratio of N_2O production to oxygen consumption in the deep ocean than in the upper ocean is required. This effect is investigated in section 5.

It is possible that some part of the mismatch between observed and modeled distributions could be due to the other model components responsible for the distribution of oceanic N_2O, namely, the circulation model and the Ocean Biogeochemistry Model, and so we also evaluate the the likelihood of these in turn. Modeled N_2O concentration at depth is affected by the circulation processes that govern abyssal ventilation (e.g., deep water formation, deep currents, convection, and mixing). A sluggish upper ocean circulation causing inadequate ventilation of the deep ocean could lead to an excess of N_2O here. The circulation model used in this study is Model P of *Toggweiler et al.* [1989a]. In that study, the authors use ^{14}C as a tracer to diagnose the model's deep ventilation processes. Comparison of the resulting deep $\Delta^{14}C$ profiles with data from the GEOSECS (Geochemical Ocean Sections Program) survey indicates that the OGCM reproduces the observations quite well. Furthermore, as is seen from Figure 9, the modeled deep AOU levels do not show a corresponding excess over the observations, a feature that would necessarily accompany a poor simulation of the surface to deep transport (assuming the biological oxygen parameterizations were also satisfactory). Thus, an incorrect modeling of deep ocean ventilation is unlikely to be the cause of the deep N_2O misfit.

The remineralization parameterizations of the OBM yield a modeled AOU profile that matches the observations well. Minor variations in magnitude, such as the mismatch of up to 30 μmol L^{-1} at intermediate depths of 1000-1500 m, have been attributed to insufficient remineralization of dissolved organic matter in this model configuration [*Anderson and Sarmiento*, 1995], and these variations by themselves are insufficient to account for the mismatches between observed and modeled N_2O. Furthermore, previous studies employing this organic matter cycling model do not give cause to believe that the remineralization parameterization is unacceptable at depth [*Anderson and Sarmiento*, 1995, *Sarmiento et al.*, 1995]. We conclude that neither the circulation model or the OBM can provide the main cause for the marked misfit between the observed and modeled ΔN_2O profiles at depth.

5. Influence of Depth Varying Processes on the Marine N_2O Source

We now examine an alternative formulation for the marine N_2O source, for which the relation between N_2O

production and oxygen consumption are based on the observed $\Delta N_2O/AOU$ ratios of *Butler et al.* [1988] and incorporate variation with depth. The depth varying process responsible could indeed be temperature, as postulated by *Elkins et al.* [1978] and *Butler et al.* [1989]. Bacterial processes often display sensitivity to temperature; in a study of factors affecting cells of Nitrosomonas Europaea, *Yoshida and Alexander* [1970] noted enhanced N_2O production as temperature was increased over a range of 15°-35°C. However, the observed correlation between marine ΔN_2O, AOU, and temperature has not been universally observed; *Oudot et al.* [1990] failed to find indications of it in regions outside biologically "active" zones in the eastern tropical Atlantic, and *Law and Owens* [1990] indicate that inclusion of temperature does not improve fits to ΔN_2O versus AOU relationships in the north Arabian Sea. Furthermore, there exist processes other than temperature sensitivity, that also vary with depth and may provide alternative explanations of the observed $\Delta N_2O/AOU$ variations. One possibility is changes in N_2O yield due to varying abundances of nitrifying and denitrifying bacteria in the water column. *Hahn* [1981] reports the results of incubation experiments by *Gundersen et al.* [1972] using seawater from various depths off the Hawaiian islands in the North Pacific. Changes in nitrate levels in ammonium enriched water samples indicate that nitrification increases with depth below 150 m, displaying a broad maximum in activity between 500-1000 m. These experiments were conducted at room temperature; hence temperature did not play a role as an influencing factor.

Another possible candidate responsible for the observed $\Delta N_2O/AOU$ depth variations is the dependence of N_2O yield from processes of nitrification and denitrification on local oxygen level. Laboratory studies have demonstrated large sensitivities in N_2O yield, especially at low oxygen concentration [*Goreau et al.*, 1980, *Jorgensen et al.*, 1984]; In addition, elevated levels of marine N_2O have been observed in suboxic waters and at the peripheries of anoxic zones [*Codispoti et al.*, 1989, *Ward et al.*, 1989]. Postulated mechanisms include processes of enhanced nitrification [*Codispoti et al.*, 1989], net N_2O production by denitrifiers at oxygen levels below 2 μmol L^{-1} [*Jorgensen et al.*, 1984], or a nitrification-denitrification couple with NO as an intermediate [*Naqvi*, 1991]. The variation of oxygen level with depth through the water column (in particular reaching anoxic and suboxic levels in such regions as the eastern equatorial Pacific and the Arabian Sea) may therefore provide an alternate explaination of the observed $\Delta N_2O/AOU$ ratios. The N_2O source formulation presented in this study accounts only for N_2O production under oxic conditions. The oxygen distribution in the OGCM does, however, produce zones of suboxic conditions in such regions as the eastern equatorial Pacific, where N_2O production would probably be better represented by the more complex cycling processes outlined above. This issue is the focus of *Suntharalingam et al.* [2000], in which we present an evaluation of the OGCM simulation of these suboxic zones, and investigate N_2O formation in and transport from these regions.

Other factors that may account for local variations in $\Delta N_2O/AOU$ ratios include mixing of water masses with different N_2O formation characteristics (such as abundances of nitrifiers or composition and availability of organic matter) [*Cohen and Gordon*, 1979], and ocurrence of local sources and sinks (e.g., assimilatory nitrate reduction or denitrification for N_2O and photosynthetic production for oxygen). In view of such possibilities as listed above, of processes that may vary with depth and not necessarily with temperature, we choose to incorporate a depth dependence in developing a global-scale N_2O source parameterization.

The *Butler et al.* [1988] measurements are primarily in the western Pacific with some stations in the East Indian Ocean. Data from the Atlantic and Indian Oceans reporting $\Delta N_2O/AOU$ variations with depth, or with other variables, are sparse. On the basis of measurements in biologically productive regions of the north eastern tropical Atlantic, *Oudot et al.* [1990] report highest $\Delta N_2O/AOU$ ratios in the oxygen minimum layer, decreasing with depth thereafter. They do not observe this behavior in measurements made outside biologically active zones. *Law and Owens* [1990] report $\Delta N_2O/AOU$ variations from measurements up to depths of 3000 m in the North Arabian Sea. They cast the observed variation in terms of two separate AOU regimes, however, reporting an almost tenfold increase in $\Delta N_2O/AOU$ ratios from low (AOU < 197 μmol L^{-1}) to high AOU (AOU > 197 μmol L^{-1}, located primarily above 1000 m) regimes. Since these measurements from other ocean basins are few, in developing an N_2O source parameterization for use on the global scale, we rely on the *Butler et al.* [1988] observations as the most extensive and consistent deepwater database available for extracting $\Delta N_2O/AOU$ variations.

5.1. Development of Depth Varying N_2O Source Formulation: Simulation N2ODZ

To parameterize the observed decrease with depth of the $\Delta N_2O/AOU$ ratios of the *Butler et al.* [1988] data we fit an exponentially decreasing function to the observations which has the form,

$$\Delta N_2O = A_o e^{\frac{(z-z_e)}{z^*}} [AOU] \tag{8}$$

where A_o and z^* are to be determined. Here z_e is the depth of the euphotic zone (119 m in the current con-

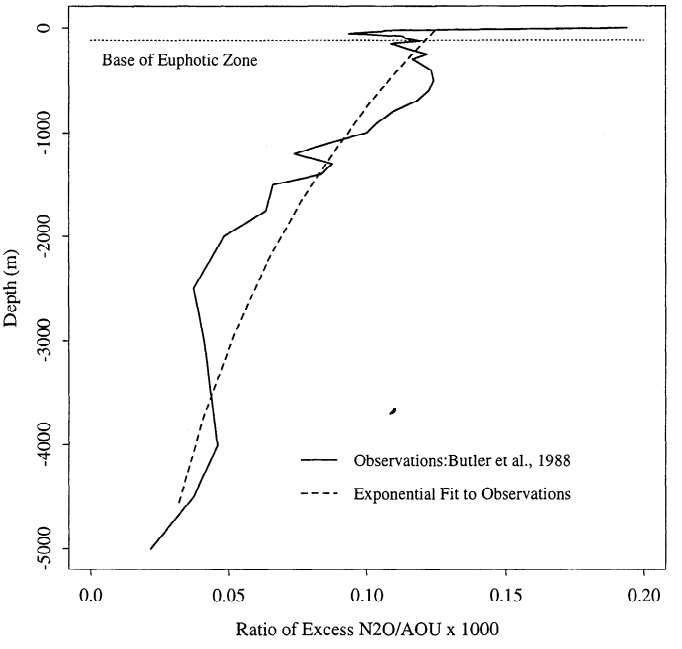

Figure 11. Fitted relationship between ΔN_2O and AOU used to parameterize the N_2O source in simulation N2ODZ. The depth dependent exponential function is fitted, by least squares minimization, to the ΔN_2O/AOU data of *Butler et al.* [1988]. The functional fit has the form, $\Delta N_2O = A_o e^{\frac{(z-z_e)}{z^*}}(AOU)$. Values derived for A_o and z^* from this fit are 0.1211×10^{-3} (mol N_2O)/(mol AOU) and 3333 m, respectively.

figuration of the OGCM). The least squares fit to the SAGA II data of *Butler et al.* [1988] is illustrated in Figure 11; the values derived for A_o and z^* from this fit are 0.1211×10^{-3} (mol N_2O)/(mol AOU) and 3333 m respectively. Thus the depth varying parameterization for the N_2O source of this simulation takes the form

$$[N_2O \text{ source}] = A_o e^{\frac{(z-z_e)}{z^*}}[O_2 \text{ consumption}] \quad (9)$$

5.2. Simulation N2ODZ: Depth Profiles

Figure 12 presents the equilibrium ΔN_2O/AOU depth profile from simulation N2ODZ and comparison with that of the Base Case and *Butler et al.* [1988] observations for the Pacific Basin. The ΔN_2O/AOU depth profile of the N2ODZ simulation shows a systematic decrease with depth and matches the structure of the observed profile far better than does the Base Case. This altered depth structure for N2ODZ results from the depth variation in the source parameterization; thus N2ODZ produces relatively more of its total N_2O source in the upper ocean and relatively less at depth, in comparison to the Base Case. As can be seen from Table 2 illustrating the distribution of the modeled N_2O source with depth, deep N_2O production (below 600 m) in N2ODZ is two-thirds that of the Base Case (i.e., 17 versus 25%) resulting in the lower deep ΔN_2O/AOU levels for N2ODZ.

The modeled ΔN_2O/AOU levels do, however, slightly underestimate the observations by about 0.02×10^{-3} below 1000 m. The small offset between observed and N2ODZ profiles below 1000 m are due to preformed oxygen effects on AOU. Model simulations indicate that the waters ventilating these deeper regions display some undersaturation in oxygen on leaving the ocean surface; the associated AOU is therefore an overestimate of biological oxygen utilization [*Suntharalingam* , 1997]. Since our N2ODZ parameterization linking the N_2O source to oxygen consumption is based directly on the ΔN_2O/AOU data and not adjusted to account for preformed oxygen, the ΔN_2O/AOU ratios derived from this model simulation are somewhat lower than the imposed biological constraint in the deep ocean. Despite this small offset, in general, this simulation serves to illustrate that the structure of the depth profiles of the *Butler et al.* [1988] data can be achieved by introducing a depth dependence into the relationship between N_2O production and oxygen consumption.

5.3. Simulation N2ODZ: Surface Fluxes

Figure 13 illustrates the distribution of zonally integrated fluxes from N2ODZ and comparison with the Base Case and observationally derived fluxes of *Suntharalingam* [1997]. Table 3 lists the fractions of the total source produced within the latitude bands 90°-

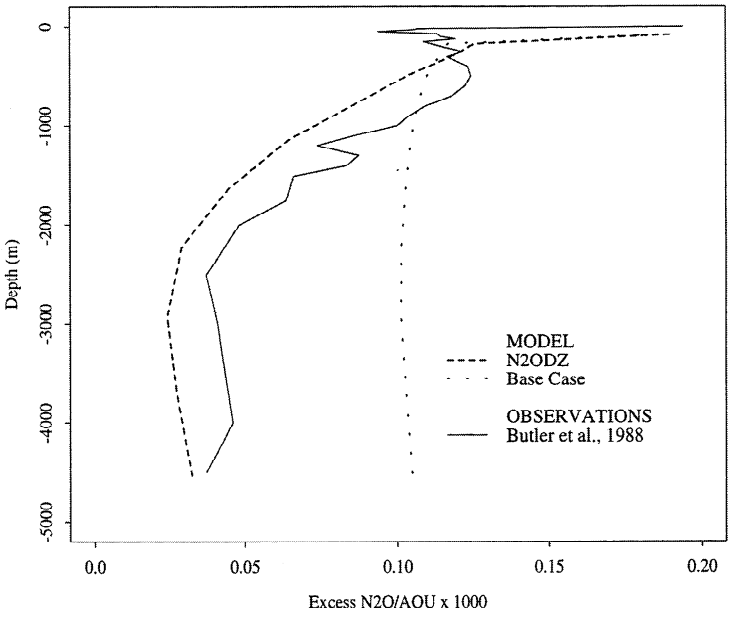

Figure 12. Variation of $\Delta N_2O/AOU$ with depth for the N2ODZ simulation and comparison with observations from *Butler et al.* [1988]. Also shown is the $\Delta N_2O/AOU$ variation with depth for the Base Case simulation. The systematic decrease with depth in the $\Delta N_2O/AOU$ ratio for N2ODZ is seen to provide a better match to the observations than does the Base Case simulation.

30°S, 30°S - 30°N, and 30°- 90°N, along with the net air-sea fluxes from these latitude belts. It should be noted that the global source derived from N2ODZ (3.85 Tg N) differs from that of the Base Case (3.65 Tg N), since different parameterizations are used to relate N_2O production to oxygen consumption in the water column. While the parameters chosen for N2ODZ are based on the *Butler et al.* [1988] data alone, that for the Base Case (i.e., α) was selected as an average of several studies relating ΔN_2O and AOU in various locations of the ocean.

The meridional flux distribution for N2ODZ does not differ significantly from the Base Case, despite arising from different vertical source distributions in the water column. As with the Base Case, the distribution is trimodal, with highest fluxes produced in the tropics and southern high latitudes. The relative insensitivity of the meridional flux distribution to the vertical structure of the source parameterization can be explained by considering that even under the Base Case formulation, the majority of the N_2O source is produced in the upper ocean (i.e., at depths above 500 m) and largely in upwelling zones. The resulting N_2O is therefore more likely to be upwelled to the surface and vented directly to the atmosphere without being subject to significant lateral transport by the deeper circulation. As indicated in Table 3, less than 13% of the total source is transported meridionally from the tropics to the high latitudes for the Base Case, and this proportion does not change significantly for N2ODZ. As was seen from Table 2, summarizing the variation with depth of the total N_2O source for the two cases, the Base Case itself produces over 75% of the global source in the upper 600 m. Thus, while shifting an additional 8% of the source

Table 2. Distribution of the Global N_2O Source With Depth: Base Case and N2ODZ Simulations.

Simulation	Global Source, %			Magnitude
	0-595 m	595-1347 m	1347-5000 m	Tg N yr^{-1}
N2ODZ	83	11	6	3.85
Base Case	75	14	11	3.65

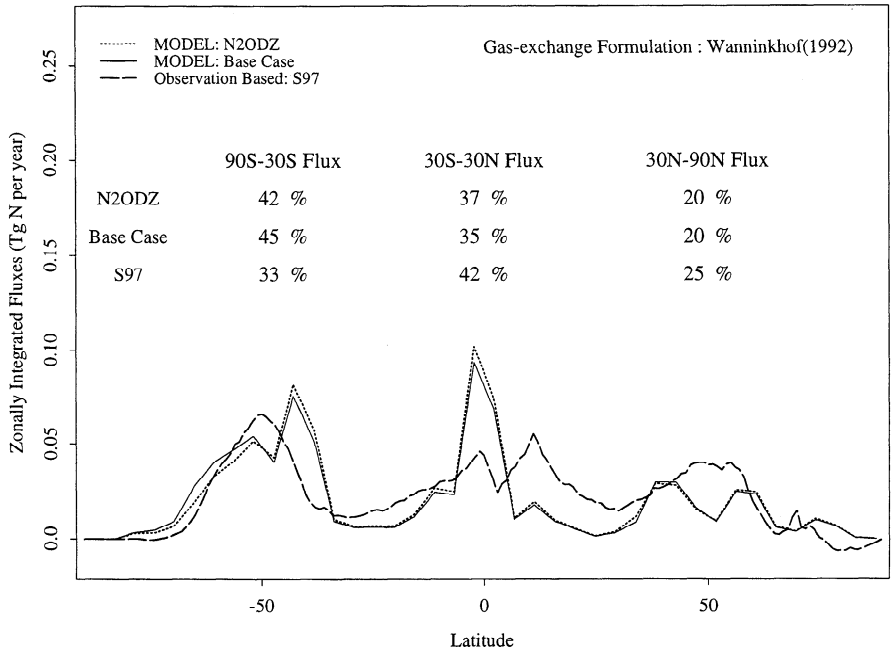

Figure 13. Zonally integrated N_2O fluxes for the N2ODZ and Base Case simulations and comparison with observation-based estimates of *Suntharalingam* [1997] (S97).

into the upper water column (for N2ODZ) produces a large decrease in the deep N_2O production and distribution, it has a relatively small effect on the upper ocean source which is the primary influence on the meridional flux distribution.

In summary, we note that as demonstrated by Figure 12, we can obtain a much better fit to the deep structure of the *Butler et al.* [1988] $\Delta N_2O/AOU$ data by employing a depth varying ratio of N_2O production to oxygen consumption in the N_2O source parameterization. The improved fit is primarily achieved by increasing the relative proportion of the N_2O source in the upper ocean. We also note, however, that since the majority of the model's N_2O production occurs in the upper ocean, em-

Table 3. Summary of the Zonally Integrated Oceanic Nitrous Oxide Source and Net Sea Air Flux by Latitude Belt, and Net Northward Transports at the 30°S and 30°N Boundaries: Base Case and N2ODZ Simulations.

Latitude Belt	Source Tg N yr^{-1}	Sea-Air Flux Tg N yr^{-1}	Northward Transport at Boundary Tg N yr^{-1}	
			30°S	30°N
N2ODZ				
90°S - 30°S	1.31 (35%)	1.65 (43%)	-0.34	
30°S - 30°N	1.92 (48.5%)	1.43 (37%)		
30°N - 90°N	0.61 (16.5%)	0.77 (20%)		0.16
Base Case				
90°S - 30°S	1.28 (35%)	1.64 (45%)	-0.36	
30°N - 30°N	1.75 (48%)	1.28 (35%)		
30°N - 90°N	0.62 (17%)	0.73 (20%)		0.11

ploying a source parameterization which produces an improved deep structure has little effect on the magnitude and distribution of surface fluxes.

6. Estimating the Magnitude of the Open Ocean N_2O Source

Global estimates of the net oceanic N_2O source have generally been calculated by two alternative methods:
1. Gas-transfer calculations: The net gas flux across the air-sea interface is estimated using extrapolated measurements of the concentration difference across the boundary in conjunction with a parameterization of the gas-transfer process. Earlier estimates were based on such parameterizations as the stagnant film model [*Bolin*, 1960, *Broecker and Peng*, 1974]. More recent estimates employ parameterizations of the gas-transfer coefficient that are based on calibrations using radiocarbon data and tracers such as sulfur-hexafluoride [e.g., *Wanninkhof*, 1992, *Liss and Merlivat*, 1986].
2. Calculations based on organic matter oxidation: These methods estimate N_2O evolution as a fraction of the nitrate regenerated during organic matter remineralization in the deep ocean, by assuming global "Redfield" type ratios relating N_2O to nitrate production [e.g., *Cohen and Gordon*, 1979, *Najjar*, 1992].

As data has accumulated, leading to an improved representation of the surface N_2O distribution as well as yielding new constraints on marine organic matter oxidation, the global estimates have diminished considerably, as illustrated by the history of flux estimates listed in Table 4. In our modeling study, marine N_2O production is driven by the magnitude and distribution of organic matter remineralization and the relationships

Table 4. Global Oceanic N_2O Flux Estimates.

Study	Flux Estimate Tg N yr^{-1}	Comments
This study	3.85 (2.7 - 8.0)	
IPCC [1995]	1 - 5	total identified sources are 10 - 17
Bange et al. [1996]	7.3-11.3	includes estimates of fluxes from estuaries, coastal waters and marginal seas.
Nevison et al. [1995]	1.2-6.8	on the basis of global extrapolation of predominantly *Weiss et al.* [1992] data
Najjar [1994]	4	on the basis of estimates of N_2O evolved during nitrification
Capone [1991]	11.25	on the basis of estimates of N_2O evolution during oceanic nitrification and denitrification
Butler et al. [1989]	1.4	estimate of El-Nino year flux, based on data from West Pacific and East Indian Oceans.
Cline et al. [1987]	$\leq$ 5.6	estimate of "normal year" (non-El Nino) flux, based on data from Equatorial Pacific
Cohen and Gordon [1979]	4 - 10	estimate based on N_2O evolved during nitrate regeneration in deep ocean
Singh et al. [1979]	11 - 17	on the basis of measurements in the Pacific
Weiss [1978]	2.8	as estimated by *Butler et al.* [1989], based on an average supersaturation of $< 4\%$.
Elkins et al. [1978]	$\leq$ 10	upper limit estimated based on oxidation considerations. Also reports an estimate of 8 Tg N yr^{-1} between $\pm$ 20°, based on data from the Central Pacific and obtained using gas-transfer method.
Hahn and Junge [1977]	45 (16 - 160)	on the basis of limited measurements in the North Atlantic

linking this to N_2O formation; that is, the source estimation method falls into the second category listed above. Net estimates of the sea-air flux are therefore not affected by the choice of gas-exchange parameterization; the primary influence of gas-exchange in these simulations is on upper-ocean N_2O concentrations and the air-sea partial pressure difference [*Suntharalingam and Sarmiento* , 1995].

The magnitude of the oceanic N_2O source derived in this study is dependent on the remineralization of the organic matter flux exported into the aphotic zone (which determines the magnitude of subsurface oxygen consumption) and the function parameterizing N_2O production as a function of oxygen consumption. As discussed in section 3.2, the organic matter cycle model partitions new production in the euphotic zone equally into particulate and dissolved organic matter pools. All the particulate organic matter sinks into the aphotic zone and is remineralized directly below its site of formation. The majority of the dissolved organic matter is also advected into the aphotic zone and remineralized there, although a portion is oxidized back into inorganic constituents in the euphotic zone itself. In this model study, nitrous oxide production is only assumed to be significant below the euphotic zone, thus the total source depends only on the "net export production", defined as that fraction of new production which is remineralized below the euphotic zone. The annual global new production of the model is 13.8 Pg C of which 11.1 Pg C constitutes the net export production remineralized in the aphotic zone.

Our "best estimate" for modeled global marine N_2O production comes from simulation N2ODZ, in which the N_2O source parameterization is based on a least squares fit to $\Delta N_2O/AOU$ ratios from the extensive *Butler et al.* [1989] data set. This yields an annual global ocean source of 3.85 Tg N. As discussed in section 2.2, reported open-ocean $\Delta N_2O/AOU$ values span a range from 0.07×10^{-3} to 0.22×10^{-3} mole N_2O/mole AOU. The estimated global N_2O source and distribution depends directly on the $\Delta N_2O/AOU$ values employed in the N_2O source model; to examine the sensitivity of model results to this variation in observations, simulations were also run incorporating these extreme $\Delta N_2O/AOU$ ratios for the parameter α in the Base Case scenario [*Suntharalingam* , 1997]. (In estimating uncertainties associated with the global source calculation, we have neglected the $\Delta N_2O/AOU$ ratios reported from the extremely oxygen-deficient regions of the Arabian Sea reported by *Law and Owens* [1990]; N_2O production in such regions is likely governed by complex cycling processes and hence not characteristic of the global ocean. The model's N_2O source changes in simple linear proportion with α to yield a range of 2.7-8.0 Tg N yr^{-1}. This range does not, however, reflect uncertainty in ocean model estimates of export production, which is more difficult to quantify. Recent OGCM estimates of export production lie in the range 11-12 Pg C yr^{-1} [*Murnane et al.*, 1999, *Yamanaka and Tajika*, 1997]; this is somewhat higher than estimates based on observations of vertical fluxes of particulate organic matter (e.g., 3-7 Pg C [*Eppley*, 1989], 8 Pg C [*Martin et al.*, 1987]) and lower than estimates based on changes in atmospheric O_2/N_2 ratios (e.g., 19 Pg C [*Keeling and Shertz*, 1992]).

We also note that the magnitude of modeled new production and remineralization (and hence the global N_2O source) is dependent on the parameterizations and processes that govern vertical transport between the surface and deep ocean. Since net productivity in the model is determined by a restoring of surface nutrient levels to the observations, excessive transport of deep nutrient rich water to the surface (for example), would result in an overestimate of new production and hence of the net N_2O source. This effect was evident in localized regions of the Southern Ocean, as discussed in section 4.1, where zones of high convection led to elevated new production and deep remineralization levels thus yielding an intense N_2O source. Finally, we note that the above estimate for the oceanic N_2O source is based only on open ocean water column oxidation of organic matter under oxic conditions. It does not include possible sources from nitrification and denitrification processes in the sediments [*Capone*, 1991, *Jorgensen et al.*, 1984], nor enhanced sources of N_2O in low oxygen regions [*Codispoti et al.*, 1992]. Furthermore, the coarse grid resolution of the OGCM does not allow us to account for contributions from estuaries and coastal regions as discussed in the study by *Bange et al.* [1996], which concluded that the extremely high supersaturations measured in such regions could potentially outweigh their small areal extent and yield significant contributions to the global flux. The omission of such factors from our model calculation suggests that our model estimate is more appropriately viewed as a lower bound on global oceanic N_2O emissions.

Accumulation of data on the marine N_2O distribution and associated cycling processes has resulted in a downward revision of the estimated oceanic flux magnitude over the past years. The range suggested by this study (2.7-8 Tg N yr^{-1}) is slightly higher than the IPCC *Houghton et al.* [1995] estimate of 1-5 Tg N, although more in accord with the *Nevison et al.* [1995] estimate of 1-7 Tg N (which was based on open ocean ΔpN_2O measurements). Two other recent studies, however, suggest considerably higher oceanic fluxes than the IPCC *Houghton et al.* [1995] range or the results of our study, namely, *Capone* [1991] (11.25 Tg N) and *Bange et al.* [1996] (7-11 Tg N). Although the open ocean component of these latter studies is more

in accord with our "best estimate" of 3.85 Tg N (i.e., 5.2 Tg N yr^{-1} [*Capone*, 1991] and 2.6-4.3 Tg N yr^{-1} [*Bange et al.*, 1996]), these studies also include significant contributions from coastal zones and estuaries.

Capone's [1991] calculation is based on estimates of oceanic N_2O evolution during processes of nitrification and denitrification accompanying organic matter remineralization in the water column and sediments. It employs global estimates of productivity in conjunction with "Redfield" type ratios relating N_2O production to nitrate cycling (i.e., assuming that N_2O production constitutes 0.3% of the nitrogen cycled via nitrification and 5% of that by denitrification) and assigns a significant role to denitrification processes in determining the magnitude of the oceanic N_2O source (i.e., suggesting that almost 70% of a total annual source of 11.25 Tg N stems from oceanic denitrification). The study by *Bange et al.* [1996], based on observations of elevated surface N_2O levels in coastal waters, marginal seas, and estuaries, suggests that N_2O fluxes from these regions are responsible for about 60% of the oceanic source. *Seitzinger and Kroeze* [1998] have recently estimated global N_2O production in freshwater and coastal marine systems, based on a global database of nitrification and denitrification rates related to external nitrogen inputs. They obtain more conservative estimates of the annual N_2O source from such marginal zones (i.e., 0.2 Tg N from estuaries and 0.6 from continental shelves). Thus, although the contribution from such regions may be lower than previously estimated, the range in the recent estimates points to a need for more measurements on N_2O formation and efflux from coastal waters and sediments in order to better evaluate their significance to the global oceanic source.

7. Summary

The primary goal of this study has been to evaluate the performance of simple parameterizations of N_2O formation in an ocean GCM, in order to see if the underlying assumptions are sufficient to explain the observed N_2O distribution. Comparison of modeled and observed surface flux distributions indicate that a scalar parameterization linking N_2O production to oxygen consumption (the Base Case scenario) is successful in reproducing the large-scale features of the observed distribution; namely, high surface supersaturations in regions of upwelling and intense biological productivity, saturation values close to equilibrium in the oligotrophic subtropical gyres, and an inverse correlation with the oxygen distribution in the oceanic interior.

Anomalous features of localized high N_2O in the southern high latitudes can be traced to characteristics of the circulation model, which produces zones of intense deep convection in these regions. The model predicts the highest proportion of the net sea-air flux to originate in the southern high latitudes, in contrast to the observational estimates of highest fluxes from the tropical latitudes. A possible cause for this disparity is model overestimation of N_2O production in the southern high latitude belt (due to elevated new production levels in the intense convective zones). We note, however, that the *Weiss et al.* [1992] database, from which the observational estimates are derived, is sparse in the southern high latitudes, and also in regions of potential significance to the oceanic N_2O flux (i.e., the eastern tropical North and South Pacific and the monsoonal upwelling region of the Arabian Sea). More comprehensive measurements are required in such regions before we can derive an observationally based global flux distribution against which we can compare the model results with full confidence.

Comparison of our simulation results with the *Butler et al.* [1988] data indicates that Base Case does not reproduce very well the deep structure of the observations. The model fails to produce the pronounced N_2O maximum in the upper ocean and overestimates levels of N_2O in the deep ocean. The most likely cause is the simplicity of the Base Case source function which postulates a constant scalar relationship between N_2O production and oxygen consumption throughout the global ocean. An alternative parameterization (N2ODZ) which accounts for processes resulting in a depth variation in the relationship between N_2O prodiction and oxygen consumption is more successful in reproducing the observed characteristics of the deep distribution. Possible factors responsible for such variations in N_2O yield include different abundances of nitrifying bacteria through the water column, sensitivity of N_2O formation processes to local oxygen level, and the influence of temperature on N_2O production. However, model results indicate that since the majority of N_2O formation occurs in the upper ocean, driven by local remineralization of organic matter (e.g., even in the Base Case scenario over 75% of the total source is formed above 600 m), this change in the vertical structure of the source parameterization has little effect on the distribution of surface N_2O fluxes.

Our "best estimate" of the global open-ocean water-column N_2O source is 3.85 Tg N yr^{-1} (range 2.7-8.0 Tg N). This range is higher than the most recent IPCC range, although it does not account for efflux from coastal waters or N_2O evolution from sedimentary processes; both these factors have recently been suggested as potentially significant influences on the oceanic flux. Finally, we note that although the simple parameterizations explored here are successful in explaining several large-scale features of the observed distribution, they do not account for more complex N_2O cycling mechanisms which may occur in suboxic and anoxic zones; the

potential global significance of such effects are further explored by *Suntharalingam et al.* [2000] and *Suntharalingam* [1997].

Acknowledgments. We thank J.R. Toggweiler, J.H. Butler and R.J. Murnane for many helpful discussions during the course of this study. We also gratefully acknowledge computer support from GFDL/NOAA through J. Mahlman. This work was supported by the U.S. Department of Energy under contract DEFG0290ER61052.

References

Anderson, L.A., and J.L. Sarmiento, Global ocean phosphate and oxygen simulations, *Global Biogeochem. Cycles, 9*, 621-636, 1995.

Bange, H.W., S. Rapsomanikis, and M.O. Andreae, Nitrous oxide in coastal waters, *Global Biogeochem. Cycles, 10*, 197-207, 1996.

Berger, W.H., Appendix, global maps of ocean productivity, In *Productivity of the Ocean: Present and Past*, edited by W.H. Berger, V.S. Smetacek, and G. Wefer, pp. 429-455, John Wiley, New York, 1989.

Bolin, B., On the exchange of CO_2 between the atmsophere and the sea, *Tellus, 12*, 274-281, 1960.

Bremner, J.M., and A.M. Blackmer, Terrestrial nitrification as a source of atmospheric nitrous oxide, edited by C.C. Delwiche, *Denitrification, Nitrification, and Atmospheric Nitrous Oxide*, pp. 151-170, John Wiley, New York, 1981.

Broecker, W.S., and T.H. Peng, Gas exchange rates between the air and sea, *Tellus, 26*, 21-35, 1974.

Butler, J.H., R.D. Jones, J.H. Garber, and L.I. Gordon, Seasonal distributions and turnover of reduced trace gases and hydroxylamine in Yaquina Bay, Oregon, *Geochim. et Cosmochim. Acta, 51*, 697-706, 1987.

Butler, J.H., J.W. Elkins, C.M. Brunson, K.B. Egan, T.M. Thompson, T.J. Conway and B.D. Hall, Trace gases in and over the West Pacific and the East Indian oceans during the El Nino Southern Oscillation event of 1987, *NOAA Data Rep. ERL ARL-16*, U.S. Dept. of Commer., Natl. Oceanic and Atmos. Admin., Boulder, Colo., 1988.

Butler, J.H., J.W. Elkins, T.M. Thompson, and K.B. Egan, Tropospheric and dissolved N_2O of the West Pacific and East Indian Oceans during the El Nino Southern Oscillation Event of 1987, *J. Geophys. Res., 94*, 14865-14877, 1989.

Bryan, B., Physiology and Biochemistry of Denitrification, in edited by C. C. Delwiche, in *Denitrification, Nitrification, and Atmospheric Nitrous Oxide*, pp.67-84, John Wiley, New York,1981.

Bryan, K., and M.D. Cox, A numerical investigation of the ocean general circulation, *Tellus, 19*, 54-80, 1967.

Capone, D.G., Aspects of the marine nitrogen cycle with relevance to the dynamics of nitrous and nitric oxide, In *Microbial Production and Consumption of Greenhouse Gases*, edited by J.E. Rogers and W.E. Whitman, pp.255-275, Am. Soc. Microbiol., Washington D.C., 1991.

Carlucci, A.F., and P. M. McNally, Nitrification by marine bacteria in low concentrations of substrate and oxygen, *Limnol. and Oceanogr., 14*, 736-739, 1969.

Codispoti, L.A., and J. P. Christensen, Nitrification, denitrification, and nitrous oxide cycling in the Eastern Tropical South Pacific Ocean., *Mar. Chem. 16*, 277-300, 1985.

Codispoti, L.A., R.T. Barber, and G.E. Friedrich, Do the nitrogen transformations in the poleward undercurrent off Peru and Chile have a globally significant influence?, in *Poleward Flows Along Eastern Ocean Boundaries, Coastal and Estuarine Studies, vol. 34*, edited by S.J. Neshyba et al., pp.281-310, Springer-Verlag, New York, 1989.

Codispoti, L.A., J.W. Elkins, T. Yoshinari, G. Fredrich, C. Sakamoto, and T. Packard, On the nitrous oxide flux from productive regions that contain low oxygen waters, in *Oceanography of the Indian Ocean*, edited by B. Desai, Oxford and IBH Pub. New Delhi, India, pp.271-284, 1992.

Cohen, Y., and L.I. Gordon, Nitrous oxide in the oxygen minima of the Eastern Tropical North Pacific: Evidence for its consumption during nitrification and possible mechanism for its production, *Deep Sea Res., 25*, 509-524, 1978.

Cohen, Y., and L.I. Gordon, Nitrous oxide production in the ocean, *J. Geophys. Res., 84*, 347-353, 1979.

Cline, J.D., D.P. Wisegarver, and K. Kelly-Hansen, Nitrous oxide and vertical mixing in the equatorial Pacific during the 1982-1983 El Nino, *Deep Sea Res., 34*, 857-873, 1987.

Crutzen, P.J., The influence of nitrogen oxides on the atmospheric ozone content, *Quart. J. R. Meteorol. Soc., 96*, 320-325, 1970.

Delwiche, T., The nitrogen cycle and nitrous oxide, In *Denitrification, Nitrification and Atmospheric Nitrous Oxide*, edited by C.C. Delwiche, pp.1-16, John Wiley, New York, 1981.

Elkins, J.W., S.C. Wofsy, M.B. McElroy, C.E. Kolb and W.A. Kaplan, Aquatic sources and sinks for nitrous oxide, *Nature, 275*, 602-606, 1978.

Eppley, R.W., New production: History, methods, problems, in *Productivity of the Ocean; Present and Past*, edited by W.H. Berger et al., pp.85-97, John Wiley, New York, 1989.

Esbensen, S.K., and Y. Kushnir, The heat budget of the global ocean : An atlas based on estimates from surface marine observations, *rep. 29*, Clim. Res. Inst., Oreg. State Univ., Cornvallis, 1981.

Goreau, T., W.A. Kaplan, S.C. Wofsy, M.B. McElroy, F.W. Valois, and S.W. Watson, Production of NO_2^- and N_2O by nitrifying bacteria at reduced concentrations of oxygen, *Appl. Environ. Microbiol., 40*, 526-532, 1980.

Gundersen, K., C.W. Mountain, D. Taylor, R. Ohye, and J. Shen, Some chemical and microbiological observations in the Pacific Ocean off the Hawaiian Islands, *Limnol. Oceanogr., 17*, 524-531, 1972.

Hahn, J., The North Atlantic Ocean as a source of atmospheric N_2O, *Tellus, 26*, 160-168, 1974.

Hahn, J., and C. Junge, Atmospheric nitrous oxide: A critical review, *Naturforsch., 32a*, 190-214, 1977.

Hahn, J., Nitrous oxide in the oceans, in *Denitrification, Nitrification and Atmospheric Nitrous Oxide*, edited by C.C. Delwiche, pp.191-240, John Wiley, New York, 1981.

Hashimoto, L.K., W.A. Kaplan, S.C. Wofsy, and M.B. McElroy, Transformations of fixed nitrogen and N_2O in the Cariaco Trench, *Deep Sea Res., 30*, 575-590, 1983.

Hellerman, S., and M. Rosenstein, Normal monthly wind stress over the world ocean with error estimates, *J. Phys. Oceanogr., 13*, 1093-1104, 1983.

Horrigan, S.G., A.F. Carlucci, and P.M. Williams, Light inhibition of nitrification in sea-surface films, *J. Mar. Res., 39*, 557-565, 1981.

Houghton, J.T., L.G. Meira Filho, J. Bruce, H. Lee, B.A. Callander, E. Haites, N. Harris, and K. Maskell, *Climate Change 1994, Radiative Forcing of Climate Change and An Evaluation of the IPCC IS92 Emission Scenarios*, Cambridge Univ. Press, New York, 1995.

Ingraham, J.L., Microbiology and genetics of denitrifiers, In *Denitrification, Nitrification and Atmospheric Nitrous Oxide*, edited by C.C. Delwiche, pp.45-66, John Wiley, New York, 1981.

Jensen, H.B., K.S. Jorgensen, and J. Sorensen, Diurnal variation of nitrogen cycling in coastal marine sediments II, Nitrous oxide emission, *Mar. Biol., 83*, 177-183, 1984.

Jorgensen, K.S., H.B. Jensen, and J. Sorensesn, Nitrous oxide production from nitrification and denitrification in marine sediment at low oxygen concentrations, *Can. J. Microbiol., 30*, 1073-1078, 1984.

Junge, C., B. Bockholt, K. Schutz, and R. Beck, N_2O measurements in air and sea water over the Atlantic, *"Meteor" Forschungsergeb., Reihe B6*, 1-11, 1971.

Keeling, R.F., and S.R. Shertz, Seasonal and interannual variations in atmospheric oxygen and implications for the global carbon cycle, *Nature, 358*, 723-727, 1992.

Kim, K.R., and H. Craig, Two-isotope characterization of N_2O in the Pacific Ocean and constraints on its origin in deep water, *Nature, 347*, 58-61, 1990.

Ko, M.K., N.D. Sze, and D.K. Weisenstein, Use of satellite data to constrain the model-calculated atmospheric lifetimes for N_2O: Implications for other trace gases, *J. Geophys. Res., 96*, 7547-7552, 1991.

Law, C.S., and N.J.P. Owens, Significant flux of atmospheric nitrous oxide from the northwest Indian Ocean, *Nature, 346*, 826-828, 1990.

Levitus, S., Climatological Atlas of the World Ocean, *NOAA Prof. Pap. 13*, Natl. Oceanic and Atmos. Admin., Silver Spring, Md., 1982.

Levitus, S., M.E. Conkright, and T.P. Boyer, World Ocean Atlas, U.S. Department of Commerce, Natl. Oceanic and Atmos. Admin., Silver Spring, Md., 1994.

Liss, P.S., and L. Merlivat, Air-sea gas-exchange rates: introduction and synthesis, in *The Role of Air-Sea Exchange in Geochemical Cycling*, edited by P. Buat-Menard, pp. 113-129, D. Reidel, Norwell, Mass., 1986.

Mahlman, J.D., H. Levy, and W.J. Moxim, Three-dimensional simulations of stratospheric N_2O: Predictions for other trace constituents, *J. Geophys. Res., 91*, D2, 2687-2707, 1986.

Martin, J.H., G.A. Knauer, D.M. Karl, and W.W. Broenkow, VERTEX: Carbon cycling in the northeast Pacific, *Deep Sea Res., 34*, 267-285, 1987.

Murnane, R., J.L. Sarmiento, and C. Le Quere, Spatial distribution of air-sea CO_2 fluxes and the interhemispheric transport of carbon by the ocean, *Global Biogeochem. Cycles, 13*, 287-306, 1999.

Najjar, R.G., Simulations of the phosphorus and oxygen cycles in the world ocean using a general circulation model, Ph.D. thesis, Princeton Univ., Princeton, N.J., 1990.

Najjar, R.G., Marine biogeochemistry, in *Climate System Modeling*, edited by K.E. Trenberth, pp.241-280, Cambridge Univ. Press, New York, 1992.

Najjar, R.G., J. L. Sarmiento, and J. R. Toggweiler, Downward transport and fate of organic matter in the oceans :Simulations with a general circulation model, *Global Biogeochem. Cycles, 6*, 45-76, 1992.

Naqvi, S.W.A., and R.J. Noronha, Nitrous oxide in the Arabian Sea, *Deep Sea Res., Part A, 38*, 871-890, 1991.

Naqvi, S.W.A., N_2O production in the ocean, *Nature, 349*, 373-374, 1991.

Naqvi, S.W.A., T. Yoshinari, D.A. Jayakumar, M.A. Altabet, P.V. Narvekar, A.H. Devol, J.A. Brandes, and L.A. Codispoti, Budgetary and biogeochemical implications of N_2O isotope signatures in the Arabian Sea, *Nature, 394*, 462-464, 1998.

Nevison, C.D., R.F. Weiss, and D.J. Erickson III, Global oceanic nitrous oxide emissions, *J. Geophys. Res., 100*, 15809-15820, 1995.

Oudot, C., C. Andrie, and Y. Montel, Nitrous oxide production in the tropical Atlantic Ocean, *Deep Sea Res., Part A, 37*, 183-202, 1990.

Pacanowski, R., K. Dixon and A. Rosati, The GFDL Modular Ocean Model Users' Guide, Geophys. Fluid Dyn. Lab., *GFDL Ocean Group Tech. Rep. 2*, Natl. Oceanic and Atmos. Admin., Princeton, N.J., 1993.

Payne, W.J., P.S. Riley, and C.P. Cox Jr., Separate nitrite, nitric oxide and nitrous oxide reducing fractions from *Pseudomonas perfectomarinus*, *J. Bact., 106*, 356-361, 1971.

Pierotti, D., and R.A. Rasmussen, Nitrous oxide measurements in the eastern tropical Pacific Ocean, *Tellus, 32*, 56-72, 1980.

Prinn, R., D. Cunnold, R. Rasmussen, P. Simmonds, F. Alyea, A. Crawford, P. Fraser, and R. Rosen, Atmospheric emissions and trends of nitrous oxide deduced from 10 years of ALE-GAGE data, *J. Geophys. Res., 95*, 18369-18385, 1990.

Ramanathan, V., R.J. Cicerone, H.B. Singh, and J.T. Kiehl, Trace gas trends and their potential role in climate change, *J. Geophys. Res., 90*, 5547-5566, 1985.

Ritchie, G.A.F., and D.J.D. Nicholas, Identification of the sources of nitrous oxide produced by oxidative and reductive processes in *Nitrosomonas europae*, *Biochem. J., 126*, 1181-1191, 1972.

Sarmiento, J.L., R. Murnane, and C. Le Quere, Air-sea CO_2 transfer and the carbon budget of the North Atlantic, *Philos. Trans. R. Soc., London, Ser.B, 348*, 211-219, 1995.

Seitzinger, S., and C. Kroeze, Global distribution of nitrous oxide production and N inputs in freshwater and coastal marine ecosystems, *Global Biogeochem. Cycles, 12*, 93-113, 1998.

Seitzinger, S., S.W. Nixon, and M.E.Q. Pilson, Denitrification and nitrous oxide production in a coastal marine ecosystem, *Limnol. Oceanog., 29*, 73-83, 1984.

Singh, H.B., L.J. Salas, and H. Shigeishi, The distribution of nitrous oxide (N_2O) in the global atmosphere and the Pacific Ocean, *Tellus, 31*, 313-320, 1979.

Suntharalingam, P., Modeling the global oceanic nitrous oxide distribution, Ph.D. thesis, Princeton Univ., Princeton, N.J., 1997.

Suntharalingam, P., J.L. Sarmiento and J.R. Toggweiler, The global significance of N_2O production and transport from oceanic low oxygen zones: a modeling study, (in press for *Global Biogeochemical Cycles*).

Suntharalingam, P., and J.L. Sarmiento, Modeling global air-sea N_2O fluxes: a sensitivity analysis of the gas-exchange formulation, in *Proceedings of the Third International Symposium on Air-Water Gas Transfer*, edited by B. Jahne and E. Monahan, AEON Verlag, Hanau, 1995.

Toggweiler, J.R., and B. Samuels, New radiocarbon constraints on the upwelling of abyssal water to the ocean's surface, in *The Global Carbon Cycle, NATO ASI Ser., Ser. I, 15*, 333-366, 1993.

Toggweiler, J.R., K. Dixon and K. Bryan, Simulations of radiocarbon in a coarse resolution world ocean model, 1:Steady state distributions, *J. Geophys. Res., 94*, 8217-8242, 1989a.

Toggweiler, J.R., K. Dixon and K. Bryan, Simulations of radiocarbon in a coarse resolution world ocean model 2:

Distributions of bomb-produced ^{14}C , *J. Geophys. Res., 94*, 8243-8264, 1989b.

Wahlen, M., and T. Yoshinari, Oxygen isotope ratios in N_2O from different environments, *Nature, 313*, 780-782, 1985.

Wanninkhof, R., Relationship between windspeed and gas exchange over the ocean, *J. Geophys. Res., 97*, 7373-7382, 1992.

Ward, B.B., H.E. Glover, and F. Lipschultz, Chemoautotrophic activity and nitrification in the oxygen minimum zone off Peru, *Deep Sea Research, 36*, 1031-1051, 1989.

Weiss, R.F., and B. A. Price, Nitrous oxide solubility in water and seawater, *Mar. Chem., 8*, 347-359, 1980.

Weiss, R.F., F. A. Van Woy, and P. K. Salameh, Surface water and atmospheric carbon dioxide and nitrous oxide observations by shipboard automated gas chromatography: results from expeditions between 1977 and 1990. *Scripps Institution of Oceanography Reference 92-11*, Scripps Inst. of Oceanogr., San Diego, Ca., 1992.

Yamanaka, Y., and E. Tajika, Role of dissolved organic matter in the marine biogeochemical cycle: Studies using an ocean biogeochemical general circulation model, *Global Biogeochem. Cycles, 11*, 599-612, 1997.

Yoshida, N., H. Morimoto, M. Hirano, I. Koike, S. Matsuo, E. Wada, T. Saino, and A. Hattori, Nitrification rates and ^{15}N abundances of N_2O and NO_3^- in the western North Pacific, *Nature, 342*, 895-897, 1989.

Yoshida, T., and M. Alexander, Nitrous oxide formation by *Nitrosomonas europae* and heterotrophic microorganisms, *Soil Sci. Soc. Am. Proc., 34*, 880-882, 1970.

Yoshida, T., and M. Alexander, Hydroxylamine oxidation by *Nitrosomonas europae*, *Soil Sci., 111*, 307-312, 1971.

Yoshinari, T., Nitrous oxide in the sea, Ph.D. thesis, Dalhousie Univ., Halifax, Nova Scotia, 1973.

Yoshinari, T., Nitrous oxide in the sea, *Mar. Chem., 4*, 189-202, 1976.

P. Suntharalingam, Department of Earth and Planetary Sciences, Harvard University, Cambridge, MA. (e-mail: pns@europa.harvard.edu)

J.L. Sarmiento, Program in Atmospheric and Oceanic Sciences, Princeton University, Princeton, NJ.

(Received July 24, 1998; revised April 28, 1999; accepted May 28, 1999.)